ISSN 2162-5298 (Print)
ISSN 2162-5301 (Online)
DOI:10.17265/2162-5298

David Publishing Company
www.davidpublisher.com

Journal of Environmental Science and Engineering A

Volume 6, Number 7, July 2017

From Knowledge to Wisdom

Journal of Environmental Science and Engineering A

Volume 6, Number 7, July 2017 (Serial Number 61)

David Publishing Company
www.davidpublisher.com

Publication Information:
Journal of Environmental Science and Engineering A (formerly parts of Journal of Environmental Science and Engineering ISSN 1934-8932, USA) is published monthly in hard copy (ISSN 2162-5298) and online (ISSN 2162-5301) by David Publishing Company located at 616 Corporate Way, Suite 2-4876, Valley Cottage, NY 10989, USA.

Aims and Scope:
Journal of Environmental Science and Engineering A, a monthly professional academic journal, covers all sorts of researches on environmental management and assessment, environmental monitoring, atmospheric environment, aquatic environment and municipal solid waste, etc..

Manuscripts and correspondence are invited for publication. You can submit your papers via Web Submission, or E-mail to environmental@davidpublishing.org, environmental@davidpublishing.com or info@davidpublishing.com. Submission guidelines and Web Submission system are available at http://www.davidpublisher.com.

Editorial Office:
616 Corporate Way, Suite 2-4876, Valley Cottage, NY 10989, USA
Tel: 1-323-984-7526, 323-410-1082
Fax: 1-323-984-7374, 323-908-0457
E-mail: environmental@davidpublishing.org; environmental@davidpublishing.com; info@davidpublishing.com

Abstracted/Indexed in:
Googel Scholar
CAS (Chemical Abstracts Service)
Database of EBSCO, Massachusetts, USA
Chinese Database of CEPS, Airiti Inc. & OCLC
Cambridge Science Abstracts (CSA)
Ulrich's Periodicals Directory
Chinese Scientific Journals Database, VIP Corporation, Chongqing, China
Summon Serials Solutions
ProQuest

Subscription Information:
Price (per year):
Print $600, Online $480
Print and Online $800

David Publishing Company
616 Corporate Way, Suite 2-4876, Valley Cottage, NY 10989, USA
Tel: 1-323-984-7526, 323-410-1082; Fax: 1-323-984-7374, 323-908-0457
E-mail: order@davidpublishing.com
Digital Cooperative Company: www.bookan.com.cn

David Publishing Company
www.davidpublisher.com

Journal of Environmental Science and Engineering A

Volume 6, Number 7, July 2017 (Serial Number 61)

Contents

Journal of Environmental Science and Engineering A 6 (2017) 329-336
doi:10.17265/2162-5298/2017.07.001

Trace Metal Contamination of Water in Naviundu River Basin, Luano and Ruashi Rivers and Luwowoshi Spring in Lubumbashi City, Democratic Republic of Congo

Bamba Bukengu Muhaya[1], Sonia Catherine Mulongo[2], Clarisse Zoza Kunyonga[3], Faustin Zigabe Mushobekwa[4] and Matthieu Kayembe wa Kayembe[5]

1. Department of Chemistry, Faculty of Science, Lubumbashi University, Lubumbashi 1825, D.R. Congo

2. Department of Geology, Faculty of Science, Lubumbashi University, Lubumbashi 1825, D.R. Congo

3. Department of Material Engineering, Higher School of Industrial Engineers, Lubumbashi University, Lubumbashi 1825, D.R. Congo

4. Department of Management, Faculty of Economics and Management, Lubumbashi University, Lubumbashi 1825, D R. Congo

5. Department of Geography, Faculty of Science, Lubumbashi University, Lubumbashi 1825, D.R. Congo

Abstract: Aluminum (Al), Vanadium (V), Chromium (Cr), Manganese (Mn), Iron (Fe), Strontium (Sr), Molybdenum (Mo), Silver (Ag), Cadmium (Cd), Tin (Sn), Caesium (Cs), Barium (Ba), Lead (Pb), Bismuth (Bi) and Uranium (U) concentrations were investigated in water samples from fifteen sampling locations in Naviundu river basin, Luano and Ruashi rivers and Luwowoshi spring in Lubumbashi city during February, March and April 2016. Chemical analyses of the samples were carried out using Inductively Coupled Plasma-Mass Spectrometer. Water pH was determined using a pH-meter and mean pH values ranged from 4.2 to 5.8. The highest mean levels of Al (5,961.954 $\mu g \cdot L^{-1}$), Pb (472.287 $\mu g \cdot L^{-1}$), V (21.014 $\mu g \cdot L^{-1}$), Cr (8.185 $\mu g \cdot L^{-1}$), U (4.163 $\mu g \cdot L^{-1}$) and Bi (0.012 $\mu g \cdot L^{-1}$) were recorded in Chemaf (Chemicals of Africa) hydrometallurgical plant effluent, those of Mn (29,714.593 $\mu g \cdot L^{-1}$), Sr (374.377 $\mu g \cdot L^{-1}$), Cd (11.358 $\mu g \cdot L^{-1}$) and Cs (0.107 $\mu g \cdot L^{-1}$) in Naviundu river at Cimenkat (Katanga's Cement Factory) exit, those of Fe (14,258.9 $\mu g \cdot L^{-1}$) and Ba (307.641 $\mu g \cdot L^{-1}$) in Luano river and those of Ag (2.669 $\mu g \cdot L^{-1}$), Mo (0.559 $\mu g \cdot L^{-1}$) and Sn (0.325 $\mu g \cdot L^{-1}$) were respectively noted in Foire channel, Naviundu river under bridge on Kasenga road and Kalulako river. The concentrations of Cd in Naviundu river at Cimenkat exit (11.358 $\mu g \cdot L^{-1}$), Chemaf hydrometallurgical plant effluent (9.697 $\mu g \cdot L^{-1}$), Naviundu river under bridge on De Plaines Avenue (6.95 $\mu g \cdot L^{-1}$) and Kalulako river (3.229 $\mu g \cdot L^{-1}$), Pb concentrations in Chemaf hydrometallurgical plant effluent (472.287 $\mu g \cdot L^{-1}$) as well as the Al, Fe and Mn concentrations recorded in most waters in this study exceeded the WHO (World Health Organization) maximum permissible limits for drinking water. The metal contamination of waters of the studied rivers, channel and spring might be partially attributed to natural processes, unplanned urbanization and poor waste management, and mostly to abandoned and ongoing mining and ore processing activities in Lubumbashi city.

Key words: Trace metal contamination, channel, river, spring, water, pH, Lubumbashi city.

1. Introduction

Industrial and artisanal mineral exploitation and ore processing activities as well as other industrial activities, urban waste, transport and agriculture contribute to the contamination of aquatic environment. Water quality deterioration from heavy metal pollution is a major issue of concern in the D.R. Congo Copperbelt, particularly given the considerable environmental legacy from 100 years of intensive industrial scale mining [1]. In the D.R. Congo Copperbelt which includes the provinces of Upper-Katanga and Lualaba, and in other eastern D.R. Congo provinces such as Ituri, North-Kivu, South-Kivu, Maniema and Tanganyika, atmosphere,

Corresponding author: Bamba Bukengu Muhaya, Ph.D., professor, research field: assessing and mapping the environmental and health impacts of abandoned mines in Sub-Saharan African countries.

soils, surface waters and groundwater are severely contaminated with trace metals and other contaminants as a result of abandoned and ongoing artisanal and industrial mining and ore processing activities [2-7]. In many locations in these provinces, mining is typically done through artisanal mining which is a small scale mining method that takes place in river beds and it can be very environmentally damaging. Artisanal mining destroys landscapes and degrades riparian zones, creating erosion and heavy silting of the water [8]. Moreover, the tailings are often dumped into the rivers and could be contaminated with mercury and cyanide, thus degrading the health of the river systems and putting the wildlife and people at risk [8-10]. In those regions, local air and soil environments, surface water and groundwater are deteriorated by factory emanations and dust from artisanal and industrial mining, tailings, discharge of untreated industrial and hospital effluents, discharge of mine water and mining wastewater into rivers, agricultural and urban runoff, and domestic wastewater [2-16]. As millions of people in those provinces largely depend on surface and groundwater to meet their domestic water needs [7, 16], the use of surface and groundwater waters heavily contaminated with trace metals represents a great risk for public health.

The current study aims to investigate trace metal contamination of waters in Naviundu river basin, Luano and Ruashi rivers and Luwowoshi spring in Lubumbashi city and to compare metal levels of the waters with the WHO (World Health Organization) guidelines for drinking-water quality [17], EPA (United States Environmental Protection Agency) drinking water standards and health advisories [18] and EU (European Union) drinking water regulations [19]. Waters of all those rivers, channel and spring are used without prior treatment by the people who live along them to meet their domestic, agricultural and recreational needs.

2. Material and Methods

2.1 Study Area and Sampling Locations

The study area encompasses various water courses of Naviundu river basin, Luwowoshi spring, Luano and Ruashi rivers in Lubumbashi city. The Naviundu river basin includes Naviundu, Kabesha, Kalulako, Kamasaka, Ma-Vallée and Mukulu rivers, Foire channel and Chemaf (Chemicals of Africa) hydrometallurgical plant effluent. Luwowoshi spring is the source of Ruashi river. Kamasaka and Mukulu rivers are tributaries of Naviundu river which is in turn a tributary of Kafubu river. All those water courses flow through Lubumbashi, the capital city of the Upper-Katanga province in south-eastern D.R. Congo (Fig. 1).

Surface water samples were collected from twelve sampling sites in the Naviundu river basin (sample and sampling site codes 21ER, 22ER, 23ER to 32ER) and from one site in each of Ruashi river (33ER), Luano river (34ER) and Luwowoshi spring (35ES) during February, March and April 2016 sampling campaigns. Of the fifteen sampling sites, five were in Naviundu river and one in each of the other rivers, channel, effluent and spring (Fig. 1). The samples were collected in clean 100-milliliter polyethylene bottles after rinsing the bottles three times with the water to be sampled. A sample code as well as the sampling site and the sampling date were written on each bottle and on the bottle lid. To prevent the sample code, sampling site and date from being erased, a transparent plastic sticker was stuck on the bottle and on its lid. Geographic coordinates of each sampling location were determined using a Garmin Etrex GPS and later on they were used for elaborating the map of sampling locations (Fig. 1).

2.2 Sample Preservation

After collection, the samples were immediately taken to the laboratory where pH was determined using

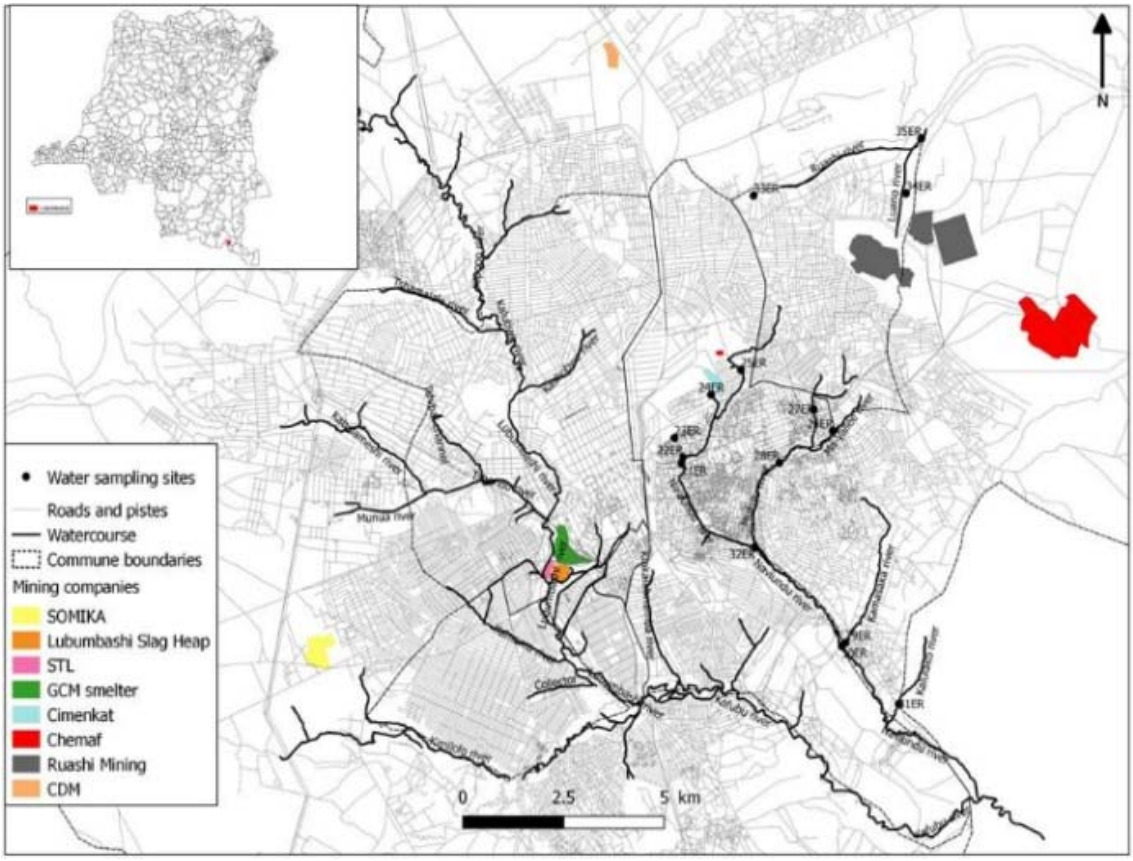

Fig. 1 Map of water sampling locations in Naviundu river basin, Luano and Ruashi rivers in Lubumbashi city during February, March and April 2016.

a pH-meter. After pH determination, samples were acidified with two to three drops of concentrated ultrapure hydrochloric acid. Then they were stored in a clean place at room temperature in the laboratory until they were analyzed for trace metals' content.

2.3 Analytical Method

The samples were analyzed using ICP-MS (Inductively Coupled Plasma-Mass Spectrometry) at the AMGC (Analytical, Environmental and Geochemical) laboratory at VUB (Vrije Universiteit Brussel) in Belgium.

3. Results and Discussion

Mean water pH values and mean water concentrations of fifteen trace metals including Ag, Al, Ba, Bi, Cd, Cr, Cs, Fe, Mn, Mo, Pb, Sr, Sn, U and V ($mg \cdot L^{-1}$) at different sampling locations as well as the WHO guidelines for drinking-water quality [17], EPA drinking water standards and health advisories [18] and EU drinking water regulations [19] are presented in Table 1. Mean water pH values were very low and ranged from 4.2 to 4.9 in Naviundu river at its confluence with Kamasaka river (4.2), Kalulako river (4.6), Naviundu river at the exit of Cimenkat (Katanga's Cement Factory) (4.7), Luano river (4.8) and Naviundu river at its confluence with Mukulu river (4.9) (Table 1 and Fig. 2). The water pH values were low in the other rivers, channel and Chemaf hydrometallurgical plant effluent and ranged from 5.1 to 5.8 (Table 1 and Fig. 2). All those water pH values were out of the WHO [17], EPA [18] and EU [19] pH range of 6.5 to 8.5 for drinking water, suggesting that waters of the studied spring, channel and rivers were improper for human consumption. Moreover, the low water pH increases metal bioavailability to aquatic

Table 1 Mean trace metal concentrations in waters (µg·L^{-1}) of the Naviundu river basin, Luano and Ruashi rivers and Luwowoshi spring in Lubumbashi city during February, March and April 2016.

Rivers, channel, spring	Sample code	pH	Sr-88 (µg·L^{-1})	Mo-98 (µg·L^{-1})	Ag-107 (µg·L^{-1})	Cd-114 (µg·L^{-1})	Sn-118 (µg·L^{-1})	Cs-133 (µg·L^{-1})	Ba-137 (µg·L^{-1})	Pb-208 (µg·L^{-1})	Bi-209 (µg·L^{-1})	U-238 (µg·L^{-1})	Al-27 (µg·L^{-1})	V-51 (µg·L^{-1})	Cr-52 (µg·L^{-1})	Mn-55 (µg·L^{-1})	Fe-56 (µg·L^{-1})
	WHO	6.5-8.5	Na	Na	Na	3	Na	Na	1,300	10	Na	30	200	Na	50	50	300
	EPA	6.5-8.5	Na	Na	100*	5	Na	Na	2,000	15	Na	30	50-200*	Na	100	50*	300*
	EU	6.5-8.5	Na	Na	Na	5	Na	Na	Na	10	Na	30	200*	Na	50	50*	200*
Naviundu river under bridge on De Plaines avenue	21ER	5.1	286.037	0.451	0.452	6.95	0.029	0.103	94.147	8.18	0.008	1.16	501.641	2.204	1.183	16,687.622	2,678.391
Naviundu river under bridge on Kasenga road	22ER	5.3	168.013	0.559	1.522	0.356	0.038	0.061	89.575	2.712	0.003	1.042	133.83	1.482	0.865	2,071.28	4,687.757
Naviundu river at Cimenkat (Katanga's Cement Factory) exit	23ER	4.7	374.377	0.238	0.311	11.358	0.008	0.107	92.431	5.607	0.005	0.886	400.5	1.731	0.797	29,714.593	962.45
Chemaf (Chemicals of Africa) hydrometallurgical plant effluent	24ER	5.8	242.301	0.329	1.86	9.697	0.068	0.082	255.788	472.287	0.012	4.163	5,961.954	21.014	8.185	2,104.966	5,152.054
Kabecha river	25ER	5.3	235.054	0.264	0.627	0.181	0.059	0.088	119.462	2.207	0.005	0.438	147.826	2.181	0.891	570.083	1,239.863
Ma-Vallée river	26ER	5.1	63.275	0.071	2.359	0.138	0.026	0.043	158.897	2.486	0.003	0.109	417.806	3.907	0.858	118.47	1,496.352
Foire channel	27ER	5.7	91.263	0.312	2.669	0.099	0.012	0.02	78.264	1.476	0.002	0.258	178.076	2.084	0.681	211.415	1,254.168
Mukulu river	28ER	5.5	30.849	0.042	1.16	0.072	0.019	0.015	40.759	0.985	0	0.095	318.921	1.273	0.449	69.596	1,044.442
Kamasaka river	29ER	5.3	138.936	0.043	2.2	1.309	0.018	0.056	85.286	3.164	0.003	0.844	572.538	3.723	1.653	2,714.81	2,056.599
Naviundu river at its confluence with Kamasaka river	30ER	4.2	31.604	0.027	0.851	0.246	0.005	0.028	41.183	3.348	0.001	0.226	601.693	3.09	0.824	154.322	3,398.445
Kalulako river	31ER	4.6	276.153	0.423	1.536	3.229	0.325	0.103	115.618	2.466	0.006	1.073	202.248	1.267	1.161	14,893.741	2,085.919
Naviundu river at its confluence with Mukulu river	32ER	4.9	41.149	0.091	0.911	0.07	0.019	0.016	29.211	0.434	0	0.139	45.121	2.137	0.339	62.228	221.785
Ruashi river	33ER	5.3	151.458	0.093	1.069	0.047	0.021	0.01	64.829	1.059	0	0.101	398.272	0.064	0.495	3,985.105	789.124
Luano river	34ER	4.8	55.064	0.029	0.96	0.365	0.003	0.071	307.641	8.846	0.001	1.15	2,329.495	6.698	1.772	3,606.887	14,258.9
Luwowoshi spring	35ES	5.8	118.378	0.193	1.226	0.133	0.09	0.031	71.578	5.188	0.002	0.31	316.923	2.196	0.944	510.649	5,098.152

* EPA Secondary Drinking Water Regulations [18], * EU Indicator Parameters [19]; EPA: United States Environmental Protection Agency Drinking Water Standards and Health Advisories, 2011 [18]; EU: European Union (Drinking-water) Regulations, 2014 [19]; Na: no available data; WHO: World Health Organization Guidelines for Drinking-Water Quality, 2017 [17].

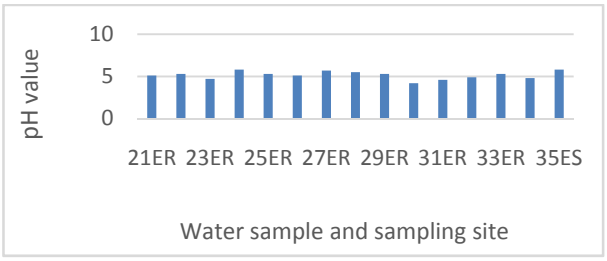

Fig. 2 Mean water pH values of water samples from Naviundu river basin, Luano and Ruashi rivers and Luwowoshi spring in Lubumbashi city during February, March and April 2016.

organisms [6, 20-25] living in the rivers, channel and spring and to human beings who depend on those waters to meet their domestic and recreational needs.

The highest mean concentrations of Al (5,961.954 $\mu g \cdot L^{-1}$), Pb (472.287 $\mu g \cdot L^{-1}$), V (21.014 $\mu g \cdot L^{-1}$), Cr (8.185 $\mu g \cdot L^{-1}$), U (4.163 $\mu g \cdot L^{-1}$) and Bi (0.012 $\mu g \cdot L^{-1}$) were recorded in Chemaf hydrometallurgical plant effluent, those of Mn (29,714.593 $\mu g \cdot L^{-1}$), Sr (374.377 $\mu g \cdot L^{-1}$), Cd (11.358 $\mu g \cdot L^{-1}$) and Cs (0.107 $\mu g \cdot L^{-1}$) were noted in Naviundu river at the exit of Cimenkat, those of Mo (0.559 $\mu g \cdot L^{-1}$) and Sn (0.325 $\mu g \cdot L^{-1}$) were found in Kalulako river, those of Fe (14,258.9 $\mu g \cdot L^{-1}$) and Ba (307.641 $\mu g \cdot L^{-1}$) were recorded in Luano river and that of Ag (2.669 $\mu g \cdot L^{-1}$) was noted in Foire channel (Table 1 and Figs. 3-6).

The mean Al (5,961.954 $\mu g \cdot L^{-1}$), Pb (472.287 $\mu g \cdot L^{-1}$), V (21.014 $\mu g \cdot L^{-1}$), Cr (8.185 $\mu g \cdot L^{-1}$), U (4.163 $\mu g \cdot L^{-1}$) and Bi (0.012 $\mu g \cdot L^{-1}$) levels of water recorded in Chemaf hydrometallurgical plant effluent were much higher than those respectively reported for Kashobwe river (5,515.816 $\mu g \cdot L^{-1}$ Al, 3.898 $\mu g \cdot L^{-1}$ Cr and 1.879 $\mu g \cdot L^{-1}$ U) and Munua river (140.294 $\mu g \cdot L^{-1}$ Pb, 12.063 $\mu g \cdot L^{-1}$ V and 0.008 $\mu g \cdot L^{-1}$ Bi) [20]. The highest mean concentration of Cd (11.358 $\mu g \cdot L^{-1}$) noted in Naviundu river at Cimenkat plant exit exceeded the WHO maximum admissible limit of 3 $\mu g \cdot L^{-1}$ in drinking-water but it was much lower than that reported for Kafubu river at its confluence with Lubumbashi river (17.994 $\mu g \cdot L^{-1}$) [20]. In the studied rivers, spring, channel and effluent, mean Mn and Fe levels of the waters were several orders of magnitude higher than the respective mean Mn and Fe levels of 49 $\mu g \cdot L^{-1}$ and 25 $\mu g \cdot L^{-1}$ noted in surface water of Komabangou, a gold mining area in the Tillabéri region, Niger [21]. The mean Pb concentrations in waters in this study (0.434 $\mu g \cdot L^{-1}$ to 472.287 $\mu g \cdot L^{-1}$) were higher than that (below quantification limit) reported for Komabangou surface water [21] and those (< 0.000 $\mu g \cdot L^{-1}$) noted in water of Luilu and Musonoie rivers, Kolwezi-Katanga (D.R. Congo) [2],

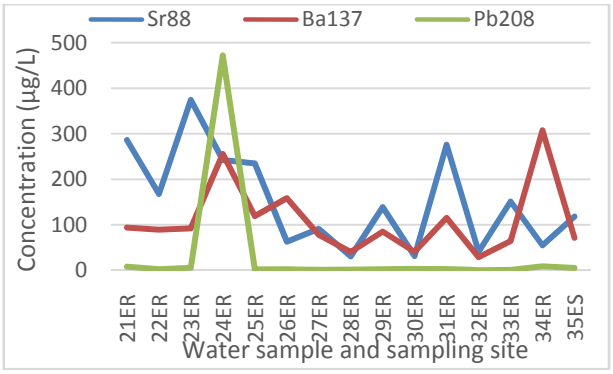

Fig. 3 Mean concentrations of Sr, Ba and Pb in water samples from Naviundu river basin, Luano and Ruashi rivers and Luwowoshi spring ($\mu g \cdot L^{-1}$) in Lubumbashi city during February, March and April 2016.

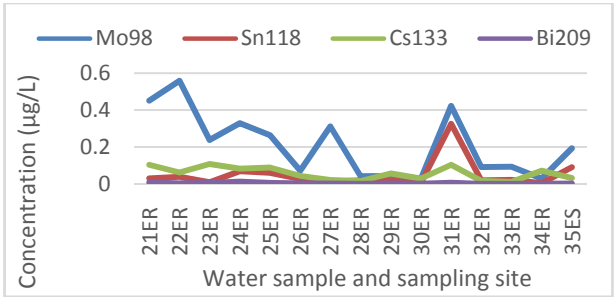

Fig. 4 Mean concentrations of Mo, Sn, Cs and Bi in water samples from Naviundu river basin, Luano and Ruashi rivers and Luwowoshi spring ($\mu g \cdot L^{-1}$) in Lubumbashi city during February, March and April 2016.

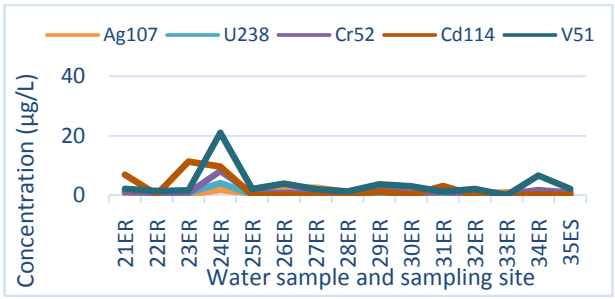

Fig. 5 Mean concentrations of Ag, U, Cr, Cd and V in water samples from Naviundu river basin, Luano and Ruashi rivers and Luwowoshi spring ($\mu g \cdot L^{-1}$) in Lubumbashi city during February, March and April 2016.

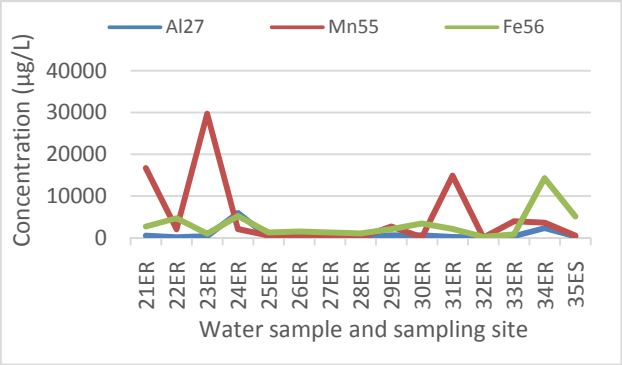

Fig. 6 Concentrations of Al, Mn and Fe in water samples from Naviundu river basin, Luano and Ruashi rivers and Luwowoshi spring (µg·L^{-1}) in Lubumbashi city during February, March and April 2016.

except for water Pb concentration at site KW13 (2,300 µg·L^{-1}) which was higher than those recorded in the present study. Also, water Pb concentration at site KW1 (100 µg·L^{-1}) [2] was higher than those recorded in this study, except for the 472.287 µg·L^{-1} noted in Chemaf hydrometallurgical plant effluent. The water Cd concentrations (0.099 µg·L^{-1} to 11.358 µg·L^{-1}) noted in this study were in the range of 0 µg·L^{-1} to 39,700 µg·L^{-1} reported for waters of the upper Lufira hydrographic basin and Tshangalele lake near Likasi (Upper-Katanga province) [3] and in that reported for Umtata river (1 µg·L^{-1} to 260 µg·L^{-1}), but they were higher than those (0.2 µg·L^{-1} to 4.3 µg·L^{-1}) reported for Mvudi river (South Africa) [16]. Water U and V levels recorded in the present study (0.095 µg·L^{-1} to 4.163 µg·L^{-1} and 0.064 µg·L^{-1} to 21.014 µg·L^{-1}, respectively) were in the ranges of 0 µg·L^{-1} to 23 µg·L^{-1} and 0 µg·L^{-1} to 36 µg·L^{-1} respectively reported for waters of upper Lufira hydrographic basin and Tshangalele lake [3]. The metal contamination of the channel and rivers of the Naviundu river basin, Luwowoshi spring and Luano and Ruashi rivers might be due to atmospheric deposition, runoff from contaminated soils and urban waste discharge and mostly to effluents from artisanal and industrial processing of ores and other industrial activities in Lubumbashi city. For the WHO guidelines for drinking-water quality, EPA drinking water standards and health advisories, and EU (drinking water) regulations [17-19], the maximum concentration limits are respectively 200 µg·L^{-1}, 200 µg·L^{-1} and 200 µg·L^{-1} for Al, 1,300 µg·L^{-1}, 2,000 µg·L^{-1} and no standard for Ba, 3 µg·L^{-1}, 5 µg·L^{-1} and 5 µg·L^{-1} for Cd, 50 µg·L^{-1}, 100 µg·L^{-1} and 50 µg·L^{-1} for Cr, 300 µg·L^{-1}, 300 µg·L^{-1} and 200 µg·L^{-1} for Fe, 50 µg·L^{-1}, 50 µg·L^{-1} and 50 µg·L^{-1} for Mn, 10 µg·L^{-1}, 15 µg·L^{-1} and 10 µg·L^{-1} for Pb and 30 µg·L^{-1}, 30 µg·L^{-1} and 30 µg·L^{-1} for U (Table 1).

Over the past decades, mining technology used in Katanga's Copperbelt region was not efficient and the resulting waste tailings still contained a relatively high level of metals [26]. Consequently, operators tended to "stockpile" these tailings behind small dams in valleys for later reprocessing. Meanwhile, the tailings became a constant source for releasing leached metals into surface waters, and most likely into groundwater as well [26]. It has also been reported that the exploitation of quartz and brick-making contribute to the remobilization of trace metals through the landscape, soil, air and water [27] and that during rainy season hydromorphic soils in the Lubumbashi city bottom valleys collect waste enriched with trace metals from various plants all around the city, from ore washing carried out by artisanal mining exploiters in their residential parcels, from malachite jewelry-making scattered in the city quarters and from a layer of slag spread on avenues to combat dust during dry season and mud during rainy season [28]. The metal-rich waste discharged into rivers and channel contributes to contaminate the receiving rivers and channel with trace metals. Thus, the metal contamination of waters of Naviundu river basin, Luano and Ruashi rivers and Luwowoshi spring might be partially due to urban and domestic effluents, runoff from metal-rich soils and mostly to abandoned and ongoing artisanal and industrial mining and ore processing activities in and around Lubumbashi city.

4. Conclusion

This study assessed trace metal contamination of

waters at twelve locations in Naviundu river basin and three locations in Luwowoshi spring, Luano and Ruashi rivers in Lubumbashi city. The results showed low mean water pH values ranging from 4.2 to 5.8 and various concentrations of Ag, Al, Ba, Bi, Cd, Cr, Cs, Fe, Mn, Mo, Pb, Sn, Sr, U and V. Naviundu river under Cimenkat (Katanga's Cement Factory) exit had the highest mean concentrations of Sr, Cd, Cs and Mn and the same river under bridge on Kasenga road had the highest Mo level with Cd and Mn levels which exceeded the WHO maximum concentration limits for drinking water.

The highest Al, Pb, Bi and U levels were found in Chemaf hydrometallurgical plant effluent with Al and Pb levels above the WHO maximum permissible limits for drinking-water. Luano river had the highest levels of Fe and Ba with Fe exceeding the WHO guideline for drinking-water and Naviundu river under bridge on Kasenga road had the highest Mo mean concentration. The trace metal contamination of waters of the studied channel, effluent, rivers and spring in Lubumbashi city might be partially attributed to natural processes, unplanned urbanization and poor waste management, and mostly to abandoned and ongoing mining and ore processing activities. It presents a risk to organisms living in those waters and to the health of the populations who depend on those rivers, channel and spring to meet their drinking water, agricultural and recreational needs.

This study recommends regular monitoring of the waters and that provincial and national authorities strictly apply the D.R. Congo Mining Regulations to avoid further deterioration of water quality and to allow full recovery of the already deteriorated water system.

Acknowledgements

Authors are thankful to Julie Mwehu for her participation in the sampling campaigns and to the AMGC Laboratory at VUB for the chemical analyses of their samples. They are grateful to Professor Martine Leermakers and Professor Willy Baeyens of the same Laboratory for having paid for the analyses as part of their support to research at Lubumbashi University in particular and in Democratic Republic of Congo in general.

References

[1] UNEP (United Nations Environment Programme). 2011. *Water Issues in the Democratic Republic of the Congo—Challenges and Opportunities.* Technical report, UNEP, Nairobi.

[2] Katemo, B. M., Colinet, G., André, L., Chocha, A. M., Marquet, J. P., and Micha, J. C. 2010. "Assessment of Food Chain Contamination with Trace Elements (Cu, Co, Zn, Pb, Cd, U, V and As) in the Upper Lufira Basin (Katanga, D.R. Congo)." *Tropicultura* 28 (4): 246-52.

[3] Atibu, E. K., Devarajan, N., Thevenon, F., Poté, J., Tshibanda, J. B., Mpiana, P. T., et al. 2013. "Concentration of Metals in Surface Water and Sediment of Luilu and Musonoie Rivers, Kolwezi-Katanga, Democratic Republic of Congo." *Applied Geochemistry* 39: 26-32.

[4] Mees, F., Maselehdani, M. N. N., De Putter, T., D'Hollander, C., Van Biezen, E., Mujinya, B. B., et al. 2013. "Concentrations and Forms of Heavy Metals around Two Ore Processing Sites in Katanga, Democratic Republic of Congo." *Journal of African Earth Sciences* 77: 22-30.

[5] Muhaya, B. B., Numbi, R. M., Lubala, F. T., Mugisho, J. B., and Tshibanda, D. K. 2015. "Heavy Metal Contamination of Well Water in the Kipushi Mining Town (Democratic Republic of Congo)." *Journal of Environmental Science and Engineering B* 4 (8): 403-18.

[6] Muhaya, B. B., Bukas, A., Lubala, F. T., Kaseti, P. K., and Mugisho, J. B. 2016. "Assessment of Trace Metals in Soils of North-Eastern Lubumbashi (Upper-Katanga Province, Democratic Republic of Congo)." *Journal of Environmental Science and Engineering A* 5 (9): 452-62.

[7] Muhaya, B. B., Kayembe, M. w. K., Kunyonga, C. Z., Mulongo, S. C., and Cuma, F. M. 2017. "Assessment of Trace Metal Contamination of Sediments in the Lubumbashi River Basin, Kafubu, Kimilolo and Kinkalabwamba Rivers in Lubumbashi City, Democratic Republic of Congo." *Journal of Environmental Science and Engineering A* 6 (4): 167-77.

[8] Wikipedia. 2017. "Mining Industry of the Democratic Republic of the Congo." Accessed September 8, 2017. https://en.wikipedia.org/wiki/Democratic_Republic_of_the_Congo.

[9] Sheppard, D. 2001. "Coltan Mining in World Heritage Sites in the Democratic Republic of Congo." The World Conservation Union, Geneva.

[10] United Nations Office for the Coordination of Humanitarian Affairs. 2002. "DRC: Two Groups Critical of Coltan Mining in the East." United Nations Office for the Coordination of Humanitarian Affairs-Integrated Regional Information Networks (IRIN), Geneva.

[11] Banza, C. L. N., Nawrot, T. S., Haufroid, V., Decree, S., De Putter, T., Smolders, E., et al. 2009. "High Human Exposure to Cobalt and Other Metals in Katanga, a Mining Area of the Democratic Republic of Congo." *Environmental Research* 109 (6): 745-52.

[12] Mohiuddin, K. M., Ogawa, Y., Zakir, H. M., Otomo, K., and Shikazono, N. 2011. "Heavy Metals Contamination in Water and Sediments of an Urban River in a Developing Country." *International Journal of Environmental Science and Technology* 8 (4): 723-36.

[13] Mubedi, J. I., Devarajan, N., Le Faucheur, S., Mputu, J. K., Atibu, E. K., Sivalingam, P., et al. 2013. "Effects of Untreated Hospital Effluents on the Accumulation of Toxic Metals in Sediments of Receiving System under Tropical Conditions: Case of South India and Democratic Republic of Congo." *Chemosphere* 93 (6): 1070-6.

[14] Cheyns, K., Nkulu, C. B. L., Ngombe, L. K., Asosa, J. N., Haufroid, V., De Putter, T., et al. 2014. "Pathways of Human Exposure to Cobalt in Katanga, a Mining Area in the D.R. Congo." *Science of the Total Environment* 490: 313-21.

[15] Kashimbo, S. K. 2016. "Influence of Surface States on the Distribution of Trace Metals in the Soil Landscape: Case of Penga-Penga (Lubumbashi, Upper-Katanga, D.R. Congo)." *International Journal of Innovation and Scientific Research* 23 (2): 326-35.

[16] Edokpayi, J. N., Odiyo, J. O., and Olasoji, S. O. 2014. "Assessment of Heavy Metal Contamination of Dzindi River, in Limpopo Province, South Africa." *International Journal of Natural Science Research* 2 (10): 185-94.

[17] WHO. 2017. *Guidelines for Drinking-Water Quality*. Fourth Edition Incorporating the First Addendum. World Health Organization, Geneva.

[18] EPA. 2011. *2011 Edition of the Drinking Water Standards and Health Advisories*. United States Environmental Protection Agency, EPA 820-R-11-002, Office of Water, Washington, DC.

[19] European Union. 2014. *EU (Drinking Water) Regulations 2014*. Statutory Instruments. S.I. No. 122 of 2014, Dublin.

[20] Muhaya, B. B., Kayembe, M. w. K., Mulongo, S. C., Kunyonga, C. Z., and Mushobekwa, F. Z. "Trace Metal Contamination of Water in the Lubumbashi River Basin, Kafubu, Kimilolo and Kinkalabwamba Rivers in Lubumbashi City, Democratic Republic of Congo." *Journal of Environmental Science and Engineering B* 6 (2): 301-11.

[21] Tidjani, D. A., Idder, T., Guero, Y., Dan Lamso, N., Matsallabi, A., Ambouta, J. M. K., et al. 2014. "Diagnostic of the Contamination of Waters by Trace Metals in the Gold Area of Komabangou—Tillabéri, Niger." *International Journal of Biological and Chemical Sciences* 8 (6): 2849-57.

[22] Violante, A., Cozzolino, V., Perolomov, L., Caporale, A. G., and Pigna, M. 2010. "Mobility and Bioavailability of Heavy Metals and Metalloids in Soil Environments." *Journal of Soil Science and Plant Nutrition* 10 (3): 268-92.

[23] Muhaya, B. B. M., Leermakers, M., and Baeyens, W. 1997. "Total Mercury and Methylmercury in Sediments and in the Polychaete *Nereis diversicolor* at Groot Buitenschoor (Scheldt Estuary, Belgium)." *Water, Air and Soil Pollution* 94 (1-2): 109-23.

[24] Baeyens, W., Meuleman, C., Muhaya, B., and Leermakers, M. 1998. "Behaviour and Speciation of Mercury in the Scheldt Estuary (Water, Sediments and Benthic Organisms)." In *Trace Metals in the Westerschelde Estuary: A Case-Study of a Polluted, Partially Anoxic Estuary*, 63-79. Springer Netherlands.

[25] Von der Heyden, C. J., and New, M. G. 2004. "Sediment Chemistry: A History of Mine Contaminant Remediation and an Assessment of Processes and Pollution Potential." *Journal of Geochemical Exploration* 82 (1): 35-57.

[26] UNEP. 2011. *The Democratic Republic of the Congo Post-Conflict Environmental Assessment Synthesis Report for Policy Makers.* United Nations Environment Programme, Nairobi.

[27] Varol, M., and Sen, B. 2012. "Assessment of Nutrient and Heavy Metal Contamination in Surface Water and Sediments of the Upper Tigris River, Turkey." *Catena* 92: 1-10.

[28] Mpundu, M. M., Yannick, U. S., Theodore, M. M., Guy, K. M., Muyembe, M., Kampanyi, I., et al. 2013. "Determination of Levels of Trace Metals in Soils of Kitchen Gardens in the Mining Town of Lubumbashi and the Risks of Contamination of Vegetable Crops." *Journal of Applied Biosciences* 65: 4957-68.

Journal of Environmental Science and Engineering A 6 (2017) 337-345
doi:10.17265/2162-5298/2017.07.002

Study of the Chemical Flooding Effect in Gao-63 Reservoir

Qiuyan Li, Xiang'an Yue, Bo Zhang, Kai Liu and Lei Yang

Key Laboratory of Petroleum Engineering, Ministry of Education, China University of Petroleum, Beijing 102249, China

Abstract: This article is aimed to discuss the impact of using two different kinds of surfactant in enhancing oil recovery in heterogeneous reservoirs. With the background of Jidong oilfield, Rui Feng surfactant which could reach ultra-low interfacial tension and combination surfactant RZ-JD80 with strong emulsifying property are chosen to do oil displacement and profile control-oil displacement experiment in homogeneous core and heterogeneous core respectively. The experiment is aimed to study the effect of oil displacement by injecting surfactant individually and the effect after injecting different profile control agent slug before surfactant flooding in heterogeneous cores. The results suggest that injecting Rui Feng surfactant and RZ-JD80 individually could enhance the oil displacement efficiency about 15 percentage points for homogeneous core. For strongly heterogeneous core, it is low efficiency by using either of these two surfactants individually. However, if injected a very little profile control agent slug before surfactant flooding, both of these two kinds of surfactant could enhance the oil recovery by different degree, especially, polymer microsphere plugging—RZ-JD80 flooding composite technology is more adaptable to Gao-63 reservoir. This technology could increase the recovery by 18.52 percentage points after surfactant flooding.

Key words: Low permeability, heterogeneous reservoir, surfactant flooding, emulsification, profile control.

1. Introduction

Most of Chinese oil fields belong to continental deposit, which are more heterogeneous than marine deposit. The Gao-63 reservoir of Jidong oilfield is a typical strongly heterogeneous reservoir [1, 2], and the permeability of some layers is low, however, in the low permeable layer, there always exists high permeable zone, which leads to seriously water channeling. In 2014, the composite water cut of produced fluid in Gao-63 reservoir has exceeded 90% and it has been in the development stage of extra high water cut stage [3, 4]. Long term water injection leads to intensified contradiction in oilfield development [5-8], so it is very urgent to research EOR (Enhanced Oil Recovery) technology adapted for the reservoir properties. Surfactant flooding, as a mature and effective EOR technique in chemical flooding, has been attracted more and more attention [9]. Its application extends from conventional medium-high permeable reservoir to high temperature and high salinity complex reservoir [10, 11]. Wang, Y., et al. [12] combined two kinds of surfactants to improve its salt resistance, obtaining good results in field test of high salinity reservoir in Zhongyuan oilfield. According to the reservoir conditions of Jin-90 block, Zhou, Q. and Liu, Y. [13] selected surfactant system to improve oil recovery in heavy oil reservoir. In recent years, the research and development of multi-functional surfactant has been the focus in China and abroad, especially the research and development of composite surfactant system is of great significance [14].

The temperature and salinity of Gao-63 reservoir are not very high, thus they are suitable for surfactant flooding. In this paper, two kinds of surfactant flooding experiments were conducted using homogeneous and heterogeneous core models to investigate the oil displacement effect of surfactant injection on homogeneous and heterogeneous core flooding. In view of heterogeneous core model, a short

Corresponding author: Qiuyan Li, Ph.D., research field: enhanced oil recovery and oilfield chemistry.

profile control agent slug is injected before surfactant flooding, and the displacement effect of profile control surface surfactant flooding technology is investigated. In addition, the plugging effect of self-developed polymer microspheres and conventional profile control agent-partially HPAM (Hydrolyzed Polyacrylamide) was compared to optimize the best development program for Gao-63 reservoir with low permeability and strong heterogeneity.

2. Material and Methods

2.1 Experimental Material

2.1.1 Experimental Equipment and Apparatus

There are many apparatus using in the experiments such as HAS-100HSB constant pressure and constant speed pump, thermostat, piston intermediate container, core holder (30 cm × 4.5 cm × 4.5 cm and 30 cm ×2.5 cm), high precision pressure sensor, Hitachi SU8010 field emission scanning electron microscopy, magnetic stirrer, ultrasonic oscillation device, RS6000 type high precision rheometer, liquid metering device, vacuum pump and some other devices.

2.1.2 Artificial Core Model

(1) Homogeneous cylindrical core model with the diameter of 2.5 cm and length of 30 cm, the permeability is 500 × 10^{-3} μm^2; (2) Heterogeneous core model (30 cm × 4.5 cm × 4.5 cm) with three layers, each thickness is 1.5 cm; permeability are 30 × 10^{-3} μm^2, 310 × 10^{-3} μm^2, 1,000 × 10^{-3} μm^2; permeability variation coefficient is 0.91. The physical parameters of core model are shown in Table 1.

2.1.3 Oil and Water Samples and Oil Displacement Agent

The experimental water is formation water of Gao-63 reservoir; total salinity is 3,260 mg/L; concentrations of Na^+/K^+, Mg^{2+}, Ca^{2+} were 1,070 mg/L, 27 mg/L and 20 mg/L; concentrations of Cl^-, HCO_3^-, SO_4^{2-} were 1,152 mg/L, 763 mg/L and 228 mg/L.

The experimental oil is a Gao-63 reservoir oil, with viscosity of 7.1 MPa·s at 77 centigrade.

Rui Feng surfactant: Light yellow, viscous liquid, soluble in water to form suspension, a kind of ultra-low interfacial tension surfactant. The oil-water interfacial tension is 7 × 10^{-3} mN/m of 0.3% mass concentration.

RZ-JD80 surfactant: in view of the target reservoir condition, with the strong emulsification ability, weak stability and the moderate low interfacial tension as the index, the compound multifunctional flooding regulation is optimized. The interfacial tension between oil and water is 6 × 10^{-2} mN/m of 0.3% mass concentration.

The high concentration polymer profile control slug is 3,000 mg/L HPAM solution.

Polymer microsphere: it can be prepared by emulsion polymerization, a certain amount of two vinyl benzene, acrylamide, Span80, azobisisobutyronitrile, AES surfactant and water [15].

2.2 Experimental Method

2.2.1 Experimental Condition

The experimental temperature of Gao-63 reservoir

Table 1 Physical parameters of core models.

Model type	Model number	Model size/cm	Permeability/× 10^{-3} μm^2	Displacement agent
Homogeneous-1	JZ-1	30 × Φ2.5	500	Rui Feng surfactant
Heterogeneous-1	FZJ-1	30 × 4.43 × 4.44	30/310/1000	
Heterogeneous-2 (HPAM)	FJZ-2 (HPAM)	30 × 4.44 × 4.45	30/310/1000	
Homogeneous-2	JZ-2	30 × Φ2.49	500	RZ-JD80
Heterogeneous-3	FJZ-3	30 × 4.42 × 4.45	30/310/1000	
Heterogeneous-4 (HPAM)	FJZ-4 (HPAM)	30 × 4.42 × 4.43	30/310/1000	
Heterogeneous-5 (Microspheres)	FJZ-5 (MP)	30 × 4.45 × 4.36	30/310/1000	

is 77 centigrade, and the displacement rate of homogeneous core is converted to 0.2 mL/min according to the oilfield development by 2.5 m/d. The displacement rate of heterogeneous core is converted to 0.5 mL/min according to the oilfield development by 1.19 m/d.

2.2.2 Emulsion Property Testing

The emulsion oil ratio is an important parameter to characterize the emulsifying properties of surfactant. The emulsifying property of surfactant is stronger and the emulsion oil ratio is higher. The mass fraction of 0.3% to measure the volume of surfactant aqueous solution and simulated oil read original oil (V_{oi}) according to the volume ratio of 1:1 added a special measuring cylinder, using ultrasonic oscillation device in 77 centigrade shocks for more than 20 minutes, the volume of residual oil (V_{or}) to readout oil-water interface stability. According to Eq. (1), the emulsion oil rate of the surfactant can be calculated:

$$R_E = \frac{V_{oi} - V_{or}}{V_{oi}} \times 100\% \quad (1)$$

wherein, R_E is emulsion oil rate; V_{oi} is initial oil volume; V_{or} is remaining oil volume.

2.2.3 Surfactant Flooding in Homogeneous and Heterogeneous Cores

For homogeneous cores and heterogeneous cores, the oil displacement experiments are carried out by using Rui Feng surfactant and RZ-JD80 surfactant, according to the program of water flooding—0.3 PV surfactant flooding—subsequent water flooding. The concrete steps are:

(1) The core is vacuumed by a vacuum pump and then the formation water and oil are saturated. At last, core is put in thermostat aging at 77 ^{o}C for more than 20 hours;

(2) Water flooding of displacement rates are 0.2 mL/min (homogeneous cores) and 0.5 mL/min (heterogeneous cores);

(3) When the water content reaches 98%, the 0.3 PV surfactant is injected;

(4) Subsequent water flooding is carried out until water content reaches 98%.

During the experiment, the injection pressure, oil and water volume, water content and recovery are recorded.

2.2.4 HPAM Profile Control—Surfactant Flooding in Heterogeneous Cores

HPAM profile control-oil displacement experiments of two kinds of surfactant are carried out according to the program of water flooding—0.1 PV 3,000 mg/L HPAM and 0.3 PV surfactant flooding—subsequent water flooding. The concrete steps are:

(1) The core is vacuumed by a vacuum pump and then the formation water and oil are saturated. At last, core is put in thermostat aging at 77 ^{o}C for more than 20 hours;

(2) Water flooding of displacement rate is 0.5 mL/min;

(3) When the water content reaches 98%, surfactant is injected until it reaches 100%;

(4) 0.1 PV 3,000 mg/L HPAM slug is injected into the core;

(5) 0.3 PV surfactant slug is injected and then subsequent water flooding is made until the water cut reaches 98%.

2.2.5 Microsphere Profile Control—RZ-JD80 Flooding in Heterogeneous Core

(1) The core is vacuumed by a vacuum pump and then the formation water and oil are saturated. At last, core is put in thermostat aging at 77 ^{o}C for more than 20 hours;

(2) Water flooding of displacement rate is 0.5 mL/min;

(3) When the water content reaches 98%, RZ-JD80 surfactant is injected until it reaches 100%;

(4) 0.1 PV polymer microspheres slug is injected into the core and temperature maintains aging for 12 hours;

(5) 0.3 PV RZ-JD80 surfactant slug is injected and then subsequent water flooding is made until the water

cut reaches 98%.

3. Results and Discussion

3.1 Emulsion Property Evaluation

Emulsification between oil and water can be realized in a variety of ways, such as oscillation, agitation, etc.. Its essence is to emulsify oil and water through the shearing action between fluid molecules. The emulsifying capacity of two kinds of surfactant and crude oil were tested by ultrasonic oscillation device, as shown in Fig. 1. For Rui Feng surfactant, there is no change between the oil-water interfaces in the initial stage of shock. A little emulsion appears near the oil-water boundary layer and the oil-water interface gradually becomes blurred after 10 minutes. With the vibration time increasing, emulsion band becomes wider and then tends to be stable and the maximum emulsion oil ratio reaches 30%. From the time of emulsion production and the final emulsion rate, the surfactant is only a weak emulsifier, which is generally emulsified. However, for RZ-JD80 surfactant, the emulsion began to produce in the early stage of vibration, and the emulsion oil ratio reached 70% at 210 seconds, then slowly increased to reach 75% at 890 seconds and remained stable. It can be seen that RZ-JD80 is a strong emulsifying agent which emulsifying capacity is very strong. Emulsification photo of two kinds of surfactant is shown in Fig. 2.

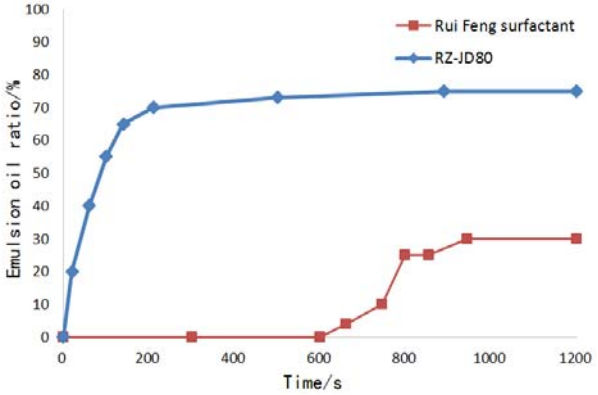

Fig. 1 Curve of emulsified oil rate.

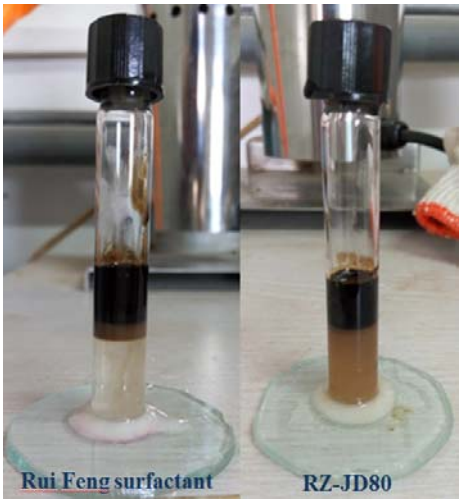

Fig. 2 Emulsification photo of crude oil.

3.2 Influence of Core Heterogeneity on Surfactant Flooding

3.2.1 Surfactant Flooding in Homogeneous Cores

For homogeneous cores, Rui Feng and RZ-JD80 surfactant flooding were carried out and the oil displacement curves are shown in Fig. 3. The water displacement efficiencies of these two experiments were 50.56% and 48.71%. With injection of two kinds of surfactant, the water content of produced liquid decreased in different degrees and the water content by Rui Feng surfactant flooding decreased to 80%. After injection of surfactant, the displacement pressure

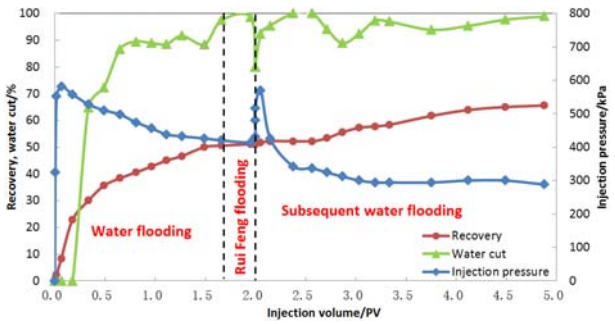

(a) Rui Feng surfactant flooding

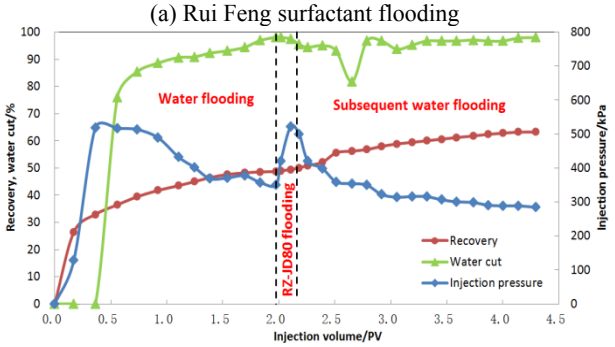

(b) RZ-JD80 surfactant flooding

Fig. 3 Curve of oil displacement in homogeneous core.

increased slightly and decreased at once, indicating that the injectivity of these two kinds of surfactant are both good. The final oil displacement efficiencies are 65.56% and 63.24% by injecting Rui Feng and RZ-JD80 surfactant. These two kinds of surfactant can increase the recovery by 15 and 14.53 percentage points respectively on the basis of water flooding. It indicated that in the homogeneous core, Rui Feng surfactant (ultra-low interfacial tension displacement agent) and RZ-JD80 surfactant (interfacial tension is not ultra-low) can basically improve the micro displacement efficiency after water flooding. The difference between the two surfactants should be reflected by improving the sweep efficiency in heterogeneous cores.

3.2.2 Surfactant Flooding in Heterogeneous Cores

The displacement effect of surfactant flooding in heterogeneous cores is shown in Fig. 4. Rui Feng surfactant can increase the recovery by 8% on the basis of water flooding and the final recovery is 47.56%. RZ-JD80 surfactant can increase the recovery by 8.95% on the basis of water flooding and the final recovery is 48.78%. It can be seen that the injection

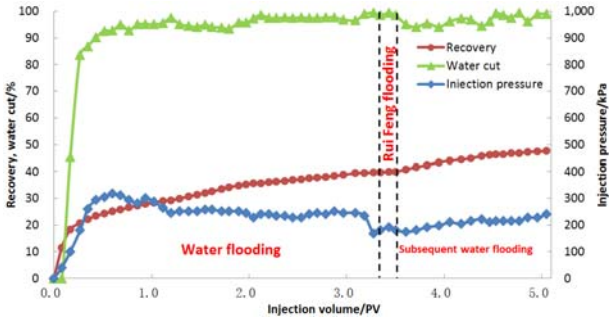

(a) Rui Feng surfactant flooding

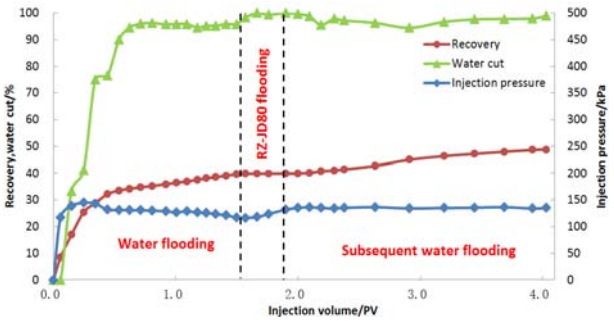

(b) RZ-JD80 surfactant flooding

Fig. 4 Curve of oil displacement in heterogeneous core.

pressure of either Rui Feng or RZ-JD80 surfactant, had not significantly increased after water flooding if surfactant solution was injected directly. Only very small amounts of emulsion could be observed in produced liquid after RZ-JD80 injection. Obviously, injected surfactant migrates mainly in water channeling or flowing channel after water flooding. It is difficult to enter the area of remaining oil with high oil saturation. In the area of low oil saturation, these two kinds of surfactant cannot make full use of its high efficiency oil displacement characteristics, especially RZ-JD80 cannot make full use of its "profile-helping" function in strong water flow area with low oil saturation. Therefore, these two types of surfactant flooding could enhance the recovery basically the same if surfactant slug is injected directly after water flooding.

3.3 Evaluation of HPAM Profile Control—Surfactant Flooding in Heterogeneous Cores

The permeability variation coefficient of heterogeneous core is 0.91. The profile control slug is 0.1 PV 3,000 mg/L HPAM solutions. Experiments were carried out by the program of HPAM profile control—0.3 PV surfactant flooding after water flooding, obtaining the oil displacement characteristic curve (Fig. 5). After profile modification, these two kinds of surfactant slug have a great difference in EOR. Rui Feng surfactant can enhance recovery by 5.39% based on surfactant flooding; however, RZ-JD80 can even enhance the recovery by 12.78% on the basis of surfactant flooding which is 2.4 times higher than Rui Feng surfactant flooding.

In the experimental scheme of profile control—surfactant flooding, the main function of surfactant slug is oil displacement and "profile-helping". Rui Feng surfactant as oil displacement agent with ultra-low interfacial tension, its main mechanism is to improve the micro displacement efficiency in swept area but the "profile-helping" function is weak. RZ-JD80 is a complex

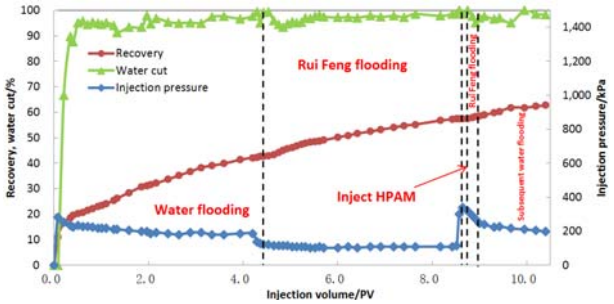

(a) HPAM profile modification—Rui Feng flooding

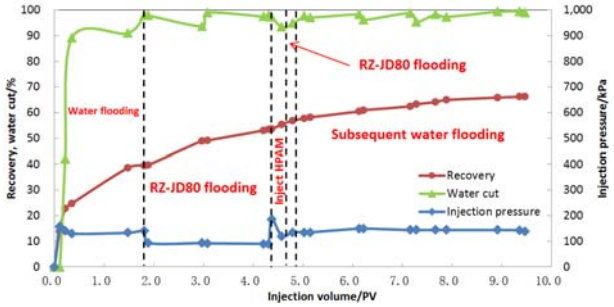

(b) HPAM profile modification—RZ-JD80 flooding

Fig. 5 Curve of HPAM plugging—oil displacement in heterogeneous core.

multifunctional flooding oil displacement—profile control agent with strong emulsifying ability, weak stability and moderate low interfacial tension. As a minute profile control slug, RZ-JD80 contact with and residual/remaining oil then generate profile control system, in situ, real-time in the process of oil migration and fine-tuning, spontaneously adjust water flooding profile, the main auxiliary slug blocking relatively small flow channel and expand the scope of the water flow channel plugging, also proving the above observed phenomenon in liquid emulsion. By contrast, Fig. 4 shows that surfactant can enter the remaining oil area as long as a small profile control slug (0.1 PV) is injected before the surfactant slug. The strong emulsified RZ-JD80 surfactant contacts with the remaining oil during the displacement process to form emulsion slug and gradually enlarges the profile control range of action. Because the strong emulsified RZ-JD80 has dual function of oil washing and profile-helping, in the experiment of HPAM profile control—surfactant flooding, utilizing RZ-JD80 as the surfactant slug can improve the recovery rate much higher than that by Rui Feng surfactant slug.

In order to research which surfactant property influences EOR the greatest, each liquid samples outlets were taken from the beginning moment of the profile after surfactant flooding. The samples of oil-water interfacial tension and emulsifying performance were tested. Test results curve as shown in Fig. 6. It can be seen that the interfacial tension of the produced liquid gradually increases with the experiment. The interfacial tension of Rui Feng increased from 9×10^{-3} mN/m to 6.02×10^{-1} mN/m while RZ-JD80's rose from 8×10^{-2} mN/m to 3.55 mN/m. The interfacial tension of Rui Feng surfactant has always been about an order of magnitude lower than that of RZ-JD80 throughout the whole experiment; the emulsion oil ratio of two kinds of surfactant flooding decreased gradually with experiment went on but decreased slightly. The emulsion oil ratio of Rui Feng decreased from 30.11% to 19.95% while RZ-JD80's decreased from 70.33% to 54.43%. During the whole experiment, the emulsion oil ratio of RZ-JD80 was far higher than that

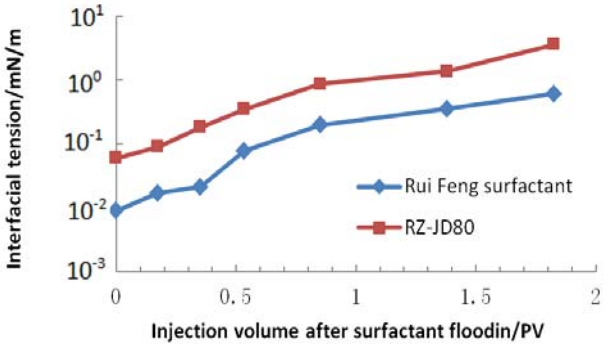

(a) Interfacial tension

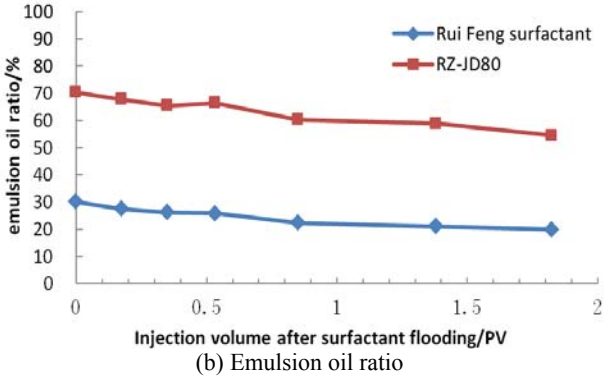

(b) Emulsion oil ratio

Fig. 6 Property curve of produced liquid.

of Rui Feng surfactant (about 2.5 times higher). According to the experimental results of profile control—oil displacement in heterogeneous cores, the enhanced recovery rate by RZ-JD80 flooding is 2.4 times higher than that by surfactant flooding. It is indicated that for Gao-63 reservoir (heterogeneous reservoir), the emulsion properties of surfactant flooding play a major role after profile control [16-19] while ultra-low interfacial tension only plays a supporting role in EOR. It also confirms the scientific design of Gao-63 reservoir flooding scheme with compound surfactant in accordance with the principle of strong emulsifying capacity and moderate low interfacial tension.

3.4 Evaluation of Polymer Microspheres Profile Control—RZ-JD80 Flooding in Heterogeneous Core

According to the experiment of RZ-JD80 flooding—0.1 PV microspheres profile control—0.3 PV RZ-JD80 flooding scheme, the displacement curve was shown in Fig. 7. Compared with the polymer slug, injection pressure can be improved significantly by microspheres plugging and maintain about 800 KPa for a long time. It could be observed the concentration of emulsion is higher in the produced liquid. It demonstrates that polymer microspheres have strong plugging ability for high permeable layer. Then the strong emulsifying agent—RZ-JD80 would be injected into medium and low permeable layers. It emulsified with residual oil in place and a profile-helping solution system with blocking capacity is generated in real time. It has played a greater role in process of oil displacement and it helps to improve both oil displacement efficiency and sweep efficiency. Compared with HPAM plugging, microspheres could increase recovery by 18.52% on basis of surfactant flooding. It shows that the adaptability of polymer microspheres plugging—RZ-JD80 flooding is better for Gao-63 reservoir (heterogeneous reservoir) with higher recovery. Summarizing Figs. 3-5 and 7, for reservoirs with less heterogeneity, improving oil displacement efficiency is the key to promote recovery; for reservoirs with more heterogeneity, improving sweep efficiency is the first step to promote recovery.

After drying the experimental core, cutting core slices (thickness is 3 mm) perpendicular to the axis of each 5 cm of the core and then scanning electron microscopy were performed. It can be observed the injected microspheres mainly concentrated within 5 cm from the entrance in high permeable layer. There are also parts of microspheres migrating to the central area of high permeable layer. However, in the middle permeable layer, only a handful of microspheres are attached to the end face. Microspheres cannot be found in low permeable layer. Photos taken by SEM (Scanning Electron Microscopy) of the high permeable layer (Fig. 8) can be clearly seen. At the core throat, the polymer microspheres with a diameter of 1-10 μm can achieve coalescence and bridging,

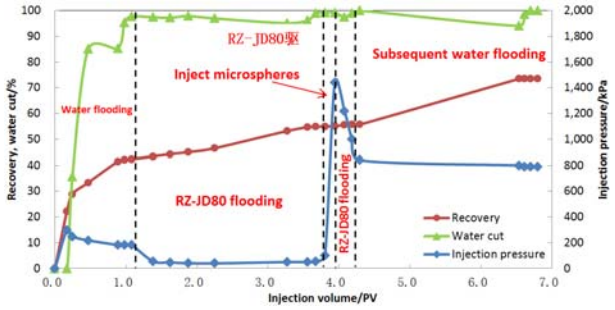

Fig. 7 Curve of microsphere plugging—oil displacement in heterogeneous core.

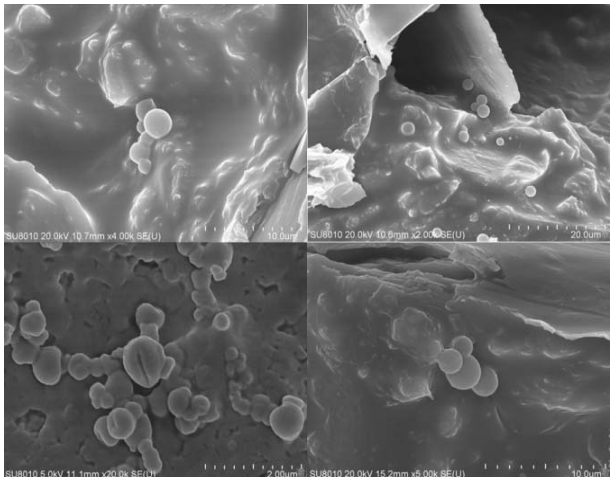

Fig. 8 SEM photographs of microspheres in core.

effectively blocking the channeling of water, enabling subsequent injection liquid diversion and entering the lower permeable layer to drive the remaining oil. It can be seen that for the heterogeneous reservoir condition of Gao-63 reservoir, profile control capacity of polymer microsphere is better and the sweep efficiency can be greatly improved as well.

4. Conclusions

For homogeneous cores, the oil displacement efficiency can be greatly improved by both of Rui Feng surfactant flooding and RZ-JD80 flooding without a profile modification slug.

For strong heterogeneous cores, enhanced oil recovery ability by only injecting two kinds of surfactant is poor. However, as long as a small profile control agent slug is injected before surfactant flooding, these two kinds of surfactant can enhance the oil recovery by different degrees.

For Gao-63 reservoir with high heterogeneity, it is not necessary to pursue ultra-low interfacial tension of surfactant for EOR. In fact, emulsifying properties play a major role, while moderate low interfacial tension can also work effectively for EOR.

The main factor restricting oil recovery in strong heterogeneous reservoirs is sweep efficiency. Profile control—surfactant flooding composite technology can greatly improve the recovery, especially the polymer microspheres—strong emulsifier flooding composite technology is very suited for Gao-63 reservoir.

References

[1] Li, H., Lin, D., and Cheng, J. 2014. "Remaining Oil Distribution Regularity Study of Complex Small Fault Block Reservoir in Extra-High Water-Cut Period in South Gaoqian Area." *Petroleum Geology and Engineering* 28 (4): 74-6.

[2] Li, Z., Lin, C., Shi, Q., Li, R., and Peng, X. 2012. "Types of Edge-Water Fault Block Reservoirs and Features of Residual Oil in the Gaoqiannan Area." *Journal of Southwest Petroleum University (Science & Technology Edition)* 34 (1): 115-20.

[3] Wang, Q. Y., Bi, Y. B., Xiu, D. Y., Fang, M. Z., and Wang, Y. H. 2013. "Research on Reservoirs and Seepage Law in Complex Fault Block Oilfield at Ultra-High Water Cut Stage." *Special Oil & Gas Reservoirs* 20 (4): 70-3.

[4] Chao, W., Fen, H., and Chao, L. 2004. "Research of Fault-Block Reservoir at High Water-Cut Stage to Enhance Development Efficiency." *Fault-Block Oil & Gas Field* 11 (4): 28-9.

[5] Li, Z., Yu, Q., and Peng, P. 1997. "A System of Methods Used for Oilfield Development during High Water-Cut Stage." *Xinjiang Petroleum Geology* 18 (4): 363-9.

[6] Huang, J., Song, X., and Meng, P. 2010. "Practice of Development Adjusting at Medium-High Water Cut Stage for Complex Small Fault-Block Oilfield." *Fault-Block Oil & Gas Field* 17 (2): 202-5.

[7] Zou, J., Yue, X., and Kong, Y. 2016. "Injection Experiment of Carbon Dioxide Flooding in Low Permeability Fissure Reservoirs." *Fault-Block Oil & Gas Field* 23 (6): 800-2.

[8] Zhang, L., Yue, X., and Yang, Z. 2015. "Immiscible Water Alternating Gas Experiments in High Temperature Heterogeneous Reservoir." *Fault-Block Oil & Gas Field* 22 (6): 776-80.

[9] Cong, W. 2017. "Research and Application of Numerical Simulation Method for Emulsion Surfactant Flooding." *Petroleum Geology and Recovery Efficiency* 24 (2): 58-62.

[10] Wang, H., Cong, X., Zheng, J., and Zhang, A. 2009. "Development and Application of Dilute Surfactant—Polymer Flooding System for Shengli Oilfield." *Journal of Petroleum Science and Engineering* 65 (2): 45-50.

[11] Zheng, Y., Huang, Q., Jiang, G., Ma, D., and Wang, Z. 2013. "Current Development and Application of Chemical Combination Flooding Technique." *Petroleum Exploration and Development* 40 (1): 96-103.

[12] Wang, Y., Li, J., and Zhao, F. 2001. "Surfactants Oil Displacement System in High Salinity Formations." In *SPE Asia Pacific Oil and Gas Conference and Exhibition*. Society of Petroleum Engineers.

[13] Zhou, Q., and Liu, Y. 2007. "Study on Increase of Oil Recovery for Jin Block 90 Using Alkali/Surfactant Compound Flooding." *Advances in Fine Petrochemicals* 8 (11): 1-5.

[14] Liu, W., Luo, L., Liao, G., Zuo, L., Wei, Y., and Jiang, W. 2017. "Experimental Study on the Mechanism of Enhancing Oil Recovery by Polymer—Surfactant Binary Flooding." *Petroleum Exploration and Development* 44 (4): 636-43.

[15] Shi, X., Yue, X., and Zhang, J. 2017. "Three-Dimensional Physical Simulation of Well Pattern

Adjusting and Deep Profile Control on Heterogeneous Reservoir after Polymer Flooding." *Fault-Block Oil & Gas Field* 24 (3): 401-4.

[16] Li, S. J., Yang, Z. Y., Song, K. P., and Kang, W. L. 2003. "Effect of Crude Oil Emulsion on Enhanced Oil Recovery in Alkaline Surfactant Polymer Flooding." *Acta Petrolei Sinica* 24 (5): 71-3.

[17] Liu, Y., Zhang, Z. H., Liao, G. Z., Yang, Z. Y., Kang, W. L., Le, J. J., et al. 2000. "The Effect of Crude Oil Emulsion on Enhanced Oil Recovery in Alkaline Surfactant Polymer Flooding." *DETERGENT & COSMETICS* 23 (supplement 1): 124-7.

[18] Lei, Z., Yuan, S., and Song, J. 2009. "Effect of Alkali-Surfactant-Polymer Emulsion on Oil Recovery." *Journal of Liaoning Technical University (Natural Science)* 28 (supplement): 77-8.

[19] Liu, P., Wang, Y., and Zheng, G. 2014. "Study of Emulsification Effect on Oil Recovery in Surfactant Flooding." *Petroleum Geology and Recovery Efficiency* 21 (1): 99-102.

Journal of Environmental Science and Engineering A 6 (2017) 346-362
doi:10.17265/2162-5298/2017.07.003

Nutritional Contribution Model of Litterfall for Adjacent Areas According to the Distance of Forest

Thomaz Costa[1], Leon Costa[2] and Letícia Almeida[2]

1. Core of Water, Soil and Environmental Sustainability (NSAM), Embrapa Milho e Sorgo, Sete Lagoas, MG 35701-970, Brazil

2. Agronomy Graduate Academy, São João Del Rei University (UFSJ), Sete Lagoas, MG 35702-031, Brazil

Abstract: The goal of this study is to evaluate the drift of litterfall from forest to adjacent areas, validate a method to estimate the drift with water balance, direction and speed of winds and quantify the nutrients of litterfall in nearby area of the forest patch as function of distance. This phenomenon can be considered an ecosystem service to improve soil quality of the agriculture crops around the forests by nutrient input coming from the litterfall. The experiment was installed in adjacent areas of the tropical forest at central region of the State of Minas Gerais, Brazil. The branches, reproductive material and leaves which fell were measured for three years into the forest and adjacents areas. The sampled nets were located on edge and equal distances from the edge. It's analyzed and estimated the contribution of the litterfall components to adjacent areas by air. The quantity of litterfall by distance had large variation between adjacent areas. And it was confirmed that model estimated the leaf drift by distance with good precision.

Key words: Wind analyze, modelling, ecosystem service.

1. Introduction

Litterfall is the organic layer deposited in forest ecosystems, with a singular role to act on the surface of the soil as an entrance and exit system, receiving first inputs through vegetation and fauna, and decomposing, supplying the roots with nutrients and organic matter. It is serving as a habitat for micro, meso and macro faunas that act in this process, and retaining and slowly releasing rainwater to the inner layers of the soil, besides contributing to the stabilization of erosion [1].

The nutrients absorbed by plants return to the soil by twigs, branches, flowers and fruits of plants and remains of animal and dead roots, and rainwater, which make up the ecosystem. This dynamic supports terrestrial ecosystems, releasing nutrients by biogeochemical and physical processes [2], and it is essential in establishing physical quality and biotic soil activity to restoration of soil fertility, especially in areas with ecological succession [3-5].

Corresponding author: Thomaz Costa, Ph.D., research field: forest science and remote sensing.

This layer deposited on the soil depends, in addition to the biomass production, on the decomposition rate of the organic matter, which varies according to the substrate composition, the activity of the decomposers and the environmental conditions, particularly temperature, humidity and soil physical properties [6]. It is known that the leaves form the largest amount in litterfall in forests, with approximately 70% of the deposited material [7-11].

The litterfall process, with rates of the deciduousness and decomposition of this material, as a key factor in the maintenance of nutrients in the ecosystem, should be more known, especially in the tropics, where there is great occurrence of soils with low levels of nutrients [12].

The amount of plant material deposited from forest ecosystems forming the litterfall is expressive, and reaches tons per hectare per year [7, 13-18]. The rate of litterfall is considered all the material deposited on the soil surface of a forest in a given period, which can be measured by deposition in collectors of pre-set sizes per unit time [19].

With information about the deposition,

accumulation and decomposition of the litter, it is possible to define strategies for the sustainable management of a given ecosystem [20]. In the investigation of the interaction of forest with areas of their surroundings, the contribution of the forest can be relevant to improve the soil quality of these areas, often used for crops with low inputs in regions with hills, mountains and saws [21].

Costa, T. C. C. and Miranda, G. A. [21] verified the drift of a semideciduous seasonal forest patch, with the potential to restore 45% Ca exported from maize crops in low input crops, 20 meters away from the patch. They concluded that the release of nutrients to the surrounding areas via air deposition of the litter is environmental service that needs better evaluation in different configurations of the physical and biotic environment.

In the case of semideciduous forest, a typology conditioned by tropical climate seasonality, with a period of intense rains and another with severe drought, the litter deposition is mainly defined by the stock of water in the soil [10]. The lower temperature can be influence, too. This typology of the Atlantic Forest also occurs as enclaves in the Savannah. When associated with wavy and strongly wavy reliefs, it is usually left in environmental reserves on the property (Legal Reserve and Permanent Preservation Areas), with adjacency to small plots of cultivated land.

The functionality of forest ecosystems is increasingly present in environmental conservation policies and in payment for ecosystem services. They contribute to the regeneration of degraded areas in their surroundings through seed dispersal, and they offer habitats for pollinators and natural enemies of pests and of disease vectors [22, 23], cycle nutrients, store water, offer food [24], protect fauna and flora, bind carbon and contribute to buffering the local climate.

In 1997, a study calculated the value of environmental services of the planet between US$ 16 and US$ 34 trillion per year. The biological control accounted for US$ 121 billion and pollination services accounted for US$ 117 billion [25]. Moreover, if some research appears with reference to the crops and forests, most likely it will have focus of the impact of crop on forest. It is the case of Duncan, D. H., et al. [26], who analyzed the impact of fertilization of crops into nearby forest patches.

In this work, authors researched an unusual focus, the possibility of forest patches of the surrounding areas to help in the maintenance of soil fertility, with deposition of plant material and releasing of nutrients provided by derives from the litterfall. Therefore, this possible kind of ecosystem service was tested.

Thus, the present work aims to measure and estimate the contribution of litter to areas adjacent to patches of seasonal semideciduous forest and validate the methodology proposed by Costa, T. C. C. and Miranda, G. A. [21] to estimate the drift considering the effect of the water balance in the deciduousness, the direction and velocity of the winds.

2. Material and Methods

The study was conducted in three adjacent areas to tropical forest patches (51, 81 and 61 codes) at the experimental farm of Embrapa Milho e Sorgo in Sete Lagoas, State of Minas Gerais, Brazil and the characteristics of the patches to adjacent areas are shown in Fig. 1.

In area 51, for receiving litterfall, 19 nets, with mesh of 2 × 2 mm and 3 meters of width with length between 10 and 35 meters, were installed on 13/07/11, from the edge of the patch, distanced 10 meters between nets (Figs. 1A and 1B). The evaluation was performed with 14 nets, because five nets were discarded for loss of quality or it was not possible to assess the origin of the contribution due to its location in relation to forest edges.

After 95 days, on 18/10/11, authors sampled litterfall deposition. They launched randomly a quadrant of 0.5 × 0.5 meters (0.25 m^2) on edge and each 5 and 5 meters, from edge of patch (Fig. 1C).

The litterfall was weighed and kept in incubator at 65 °C until stabilization to obtain the dry weight (g/m^2). Authors had maintenance problem with this experiment. The conduction of the test was possible in the dry season after scraping soil, desiccation, mowing and weeding. During the rainy season, the growth of grasses and weeds lifted nets, precluding the maintenance and continuity of the evaluation.

In area 81, for receiving litterfall, collectors with 1 m^2 of area and height of 1 m of the terrain were used, total of the 17 nets, 5 into the patch and 12 on adjacent area, subdivided in three lines spaced of 10 meters, of 4 nets (0, 5, 10 and 15 meters of the patch, Figs. 1D and 1E).

The litterfall was collected on days 27/08/14, 26/09/14, 28/10/14, 26/11/14, 23/12/14, 29/01/15, 27/02/15 27/03/15, 29/04/15, 27/05/15, 28/06/15 and 28/07/15.

The collected material was separated on brunch, reproductive material and leaves, and the dry weight (g/m^2) was obtained with the same routine of the 51 area.

In area 61, the same material was used (Fig. 1F). The difference is that the nets in adjacent area were distant 3, 8, 13 and 18 meters of the patch. The litterfall was collected on 28/08/2015, 30/09/2015, 30/10/2015, 30/11/2015, 29/12/2015, 29/01/2016, 26/02/2016, 28/03/2016, 28/04/2016, 30/05/2016, 30/06/2016 and 29/07/2016.

Inside the patch in area 51, the monitoring of litter deposition was performed through 10 nets deployed in two plots of 20 × 20 m on periods: 15/07/11, 15/08/11, 13/09/11, 18/10/11, 16/11/11, 14/12/11, 16/01/12, 14/02/12, 15/03/12, 15/04/12, 14/05/12, 15/06/12 and 15/07/12. The leaves of material that formed litter were monthly collected and weighed. The same routine was performed to patches 81 and 61 on its collect periods respectively, with following differences: five nets in one plot of 20 × 20 m were used for each patch and litterfall was separated in branches, reproductive material and leaves.

The collected leaves in each patch were split between dry and moist periods and ground and mixed for leaf analysis of macro (N, P, K, Ca and Mg) and micronutrients (Zn, Fe, Mn and Cu). It is used the content of dry and moist with dry weight of the correspondent periods.

The water balance of Thornthwaite was calculated with daily data of PET (Potential Evapotranspiration) by Penman-Monteith [27, 28], and the precipitation, with data obtained from the climatologic station of the INMET (National Institute of Meteorology), installed at the Embrapa Experimental Farm, distant around 6 km and 8 km of study areas. In order to calculate the daily water excess and the water deficiency, an available water capacity of 150 mm was used and the methodology described by Pereira, A. R., et al. [28] was carried out by the development of a VBA (Visual Basic for Application) routine [13]. The data were summed for the periods of leaves collecting in each area.

Into the patch, the period is considered for the estimation of the drift on adjacent area. It reflects the influence of the water balance on the deciduousness, caused by the climatic seasonality. This phenomenon can be associated with a second-degree polynomial model. With this model, using data of 2011/2012 [13], it recorded a minimum point between the end of February and the beginning of March. The September was the period with more fall of leaves.

The estimated litter drift by distance from the forest patch was obtained as: a reference period with observed data was chosen (August, September and October). This period was used by means of weighting factors between this and the other periods, which will be estimated. This weight is water balance influence on deciduousness.

For the influence of drifting wind, frequency tables by UTC (Universal Time Coordinated) time are used. The wind data obtained from the INMET weather station were organized into four frequency tables, 2 for speed ($m \cdot s^{-1}$), and 2 for direction, for each UTC time,

Fig. 1 Distribution of nets in the adjacent areas of forest at Embrapa Milho e Sorgo Farm and way of collection: (A) orbital view (Ikonos Image/Google Earth); (B) net detail; (C) quadrant of 0.5 × 0.5 m randomly sampled in the edge, and distances of 5, 10, 15, 20, 25, 30 and 35 meters from the edge of the patch to litter collection in area 51; (D) layout of second experiment (area 81); (E) viewer of nets local; (F) layout of third experiment (area 61).

12, 18 hours. The time 24 hours was not used because the night collect was disabled during experiment. The unfavorable winds for litter drift in the surrounding area and days with lull were treated as no effective in the direction analysis. Because of the defect on anemometer, the lack of wind data occured in January and February 2012. This lack was filled with 2011 data.

For the wind speed tables (12 hours and 18 hours), a factor per period (Fw_p) is generated. Fw_p is weighted average that is calculated by the wind speed (w_i) multiplied by its frequency of occurrence (f_i), and divided by the total frequency (f_t). n is the number of wind speeds occurring in the period (Eqs. (1) and (2)).

$$Fw_p = \sum_{i=1}^{n} \frac{w_i * f_i}{f_t} \quad (1)$$

$$f_t = \sum_{i=1}^{n} f_i \quad (2)$$

This factor, compared between periods, indicates the greater or lesser influence of the wind speed in the drift.

In the direction tables, the winds that drift litter to the adjacent area were chosen by position. The factor per period in this case is the ratio between the sum of favorable wind frequencies (j) and the total frequency, including the lull (C) (Eqs. (3) and (4)).

$$Fw_p = \sum_{j=1}^{nv} \frac{f_j}{f_t} \quad (3)$$

$$f_t = \sum_{j=1}^{n} f_j \quad (4)$$

To estimate the dry weight (whd) at the edge of the patch, the proportionality ratio between the period to be estimated and the reference period is used, with the water balance factor ($whd_{edge\ [ref.]}/whd_{frag\ [ref.]}$) and the wind factor ($Fw_{[period.]}/Fw_{[ref.]}$), expressed in Eq. (5).

$$\frac{whd_{edge[period]}}{whd_{frag[period]}} = \frac{whd_{edge[ref]}}{whd_{frag[ref]}} * \frac{Fw_{[period]}}{Fw_{[ref]}} \quad (5)$$

To estimate the dry weight (whd) of each litter component at the edge of the patch (0 m) in each period, this term is isolated in Eq. (6):

$$whd_{edge[period]}(g.m^{-2}) = whd_{frag[period]} * \frac{whd_{edge[ref]}}{whd_{frag[ref]}} * \frac{Fw_{[period]}}{Fw_{[ref]}} \quad (6)$$

For the estimation of the whd at distances per period, the proportionality between the distance whd and the edge whd (0 m) in the reference period was used, with the distance whd to estimate and the whd of the edge of the period, estimated by Eq. (6).

All estimates, edge and distances are obtained by wind-frequency table, and the final whd ($g \cdot m^{-2}$) value is obtained by the arithmetic mean per period among the 4 tables: speed wind to 12 h and 18 h and direction wind to 12 h and 18 h.

Through leaf analysis of macro and micro nutrients of leaf litter collected in the inner forest patch, the amount of nutrients deposited on period and one year by distance was estimated. In case of area 51, which did not separate the litterfall in branches, reproductive material and leafs, this estimate is possible because the nutrient content in the leaves compared to those found in the forming material litter did not vary much [10, 11].

The amounts of nutrients deposited in the soil were compared with data of exportation of nutrients for maize in productivity level with low input use.

3. Results

Table 1 shows the first characteristics about areas 51, 81 and 61. The areas 51 and 61 have the similar canopy (LAI, D, B) and hydric (DstWat, ElevWat) parameters, except for soil class and typology. In area 81, a river crosses with distance of 160 meters from the site, with altitude differences of 12 meters (Table 1), which gives the patch the classification of evergreen forest [29]. In areas 51 and 61, in which the patches are classified as semi deciduous seasonal forest, the river is 550 and 720 meters respectively away from the site [29].

Table 2 shows the correlations between climatic variables and leaf deposition. It is verified that the deciduousness increases with the reduction of the minimum temperature, the relative humidity and the rain, with the increase of the evapotranspiration, that reflects in the increase of the water deficit and reduction of the water surplus, conditions that characterize the dry season. In this region, it generally starts from March to April and ends from September to October. Wind influences the deciduous, especially in the hot times of the day, with greater turbulence of the atmosphere. These are the drive variables of leaf deposition in semi deciduous and deciduous forests, which can be summarized in the deficiency and surplus water, velocity and direction of the patch winds to adjacent areas.

The water balance shows that deciduousness declines with water surplus. In Fig. 2, the graphics on the right show variation of the leaves deposition within the patch by period. The lower rates of deciduousness are due to senescence of leaves and the influence of wind and small periods without rain in

Table 1 Location, canopy and diversity parameters by site: LAI (Leaf Area Index); average tree height on edge canopy (h); density of individuals (D); basal area (B); Shannon index (H'); slope; distance of the water body (DstWat); elevation difference between the site and the water body (ElevWat); soil classes and forest typology of sites.

Site	51	81	61
Coordinates	44º09'33.45" O 19º26'00.42" S	44º09'24.73" O 19º25'53.91" S	44º08'54.91" O 19º24'54.38" S
LAI (m^2 of leaves and m^{-2} of ground)	4.4	5.3	4.2
h (m)	19 ± 3.48	18 ± 1.64	9 ± 1.59
D ($ind \cdot m^{-2}$)	0.09	0.18	0.09
B ($m^2 \cdot ha^{-1}$)	26	32	20
H'	2.64	2.87	2.47
Slope (degree)	0-20º	0-7º	3-11º
DstWat (m)	550	160	720
ElevWat (m)	10	12	25
Soil class	Typical distrofic yellow argissol	Typical hummic atrophic cambissol	Typical hummic distrofic cambissol
Tipology by usual method [29]	Semideciduous	Evergreen florest	Deciduous

Table 2 Pearson correlation matrix between climatic variables and leaf dry weight in the respective collection periods for areas 51, 81 and 61. Note 1: The averages were considered by period for the maximum, minimum and average temperatures in degrees Celsius (TMax, Tmin and Tmd), % relative humid at 12 h and 18 h (UR12, UR18), wind velocity (m/s) at 12 h and 18 h (V12, V18), and the cumulative, in mm in the period, for precipitation, potential evapotranspiration, water deficiency and surplus (PP, ET0, DEF and EXC). Dry leaf deposition is in $g \cdot m^{-2}$ (leaf). Values in bold are different from 0 with a significance level alpha = 0.05 (n = 36).

Variables	TMax	TMin	Tmd	UR12	UR18	PP	ET0	DEF	EXC	V12	V18
TMin	**0.54**										
Tmd	0.28	**0.41**									
UR12	**-0.56**	0.27	-0.16								
UR18	**-0.33**	**0.56**	0.01	**0.92**							
PP	0.03	**0.64**	0.23	**0.58**	**0.72**						
ET0	**0.61**	-0.05	**0.35**	**-0.89**	**-0.78**	**-0.38**					
DEF	-0.31	**0.35**	-0.17	**0.86**	**0.83**	**0.47**	**-0.89**				
EXC	-0.07	**0.47**	0.12	**0.57**	**0.65**	**0.95**	**-0.40**	**0.43**			
V12	**0.35**	-0.13	0.25	**-0.75**	**-0.60**	**-0.38**	**0.73**	**-0.73**	**-0.42**		
V18	0.03	**-0.37**	0.03	**-0.49**	**-0.54**	-0.27	**0.44**	**-0.53**	-0.24	**0.68**	
Dry leaf	-0.23	**-0.74**	-0.15	**-0.48**	**-0.62**	**-0.48**	**0.39**	**-0.57**	**-0.37**	**0.38**	**0.52**

the summer season.

The data sums branches, reproductive material (flowers, fruits and seeds) and leaves, in $g \cdot m^{-2}$ by distance on areas 51, 81 and 61, are show in Figs. 3A, 3B and 3C, respectively. Fig. 3A is two dimensions because in this area only one period of 95 days was collected. Fig. 3 shows litterfall deposited in greater quantity at edge of the patch. The leaves and flowers reach greater distances due to lower weights.

Comparing the areas (it is necessary to divide values of area 51 by 3, approximately because of period 3 months and three days), area 51 had major supply of litterfall followed by area 81, and the area 61 had minor contribution.

In area 51, the collect method was different, the nets stayed on level of terrain and the area is more surrounded by vegetation (Fig. 1). In addition, the favorable conditions for litter drift refer to the higher slope of the terrain, with an inclined plane towards the collectors, reaching 20% of slope. These conditions can be contributing to more quantity of deposition litterfall.

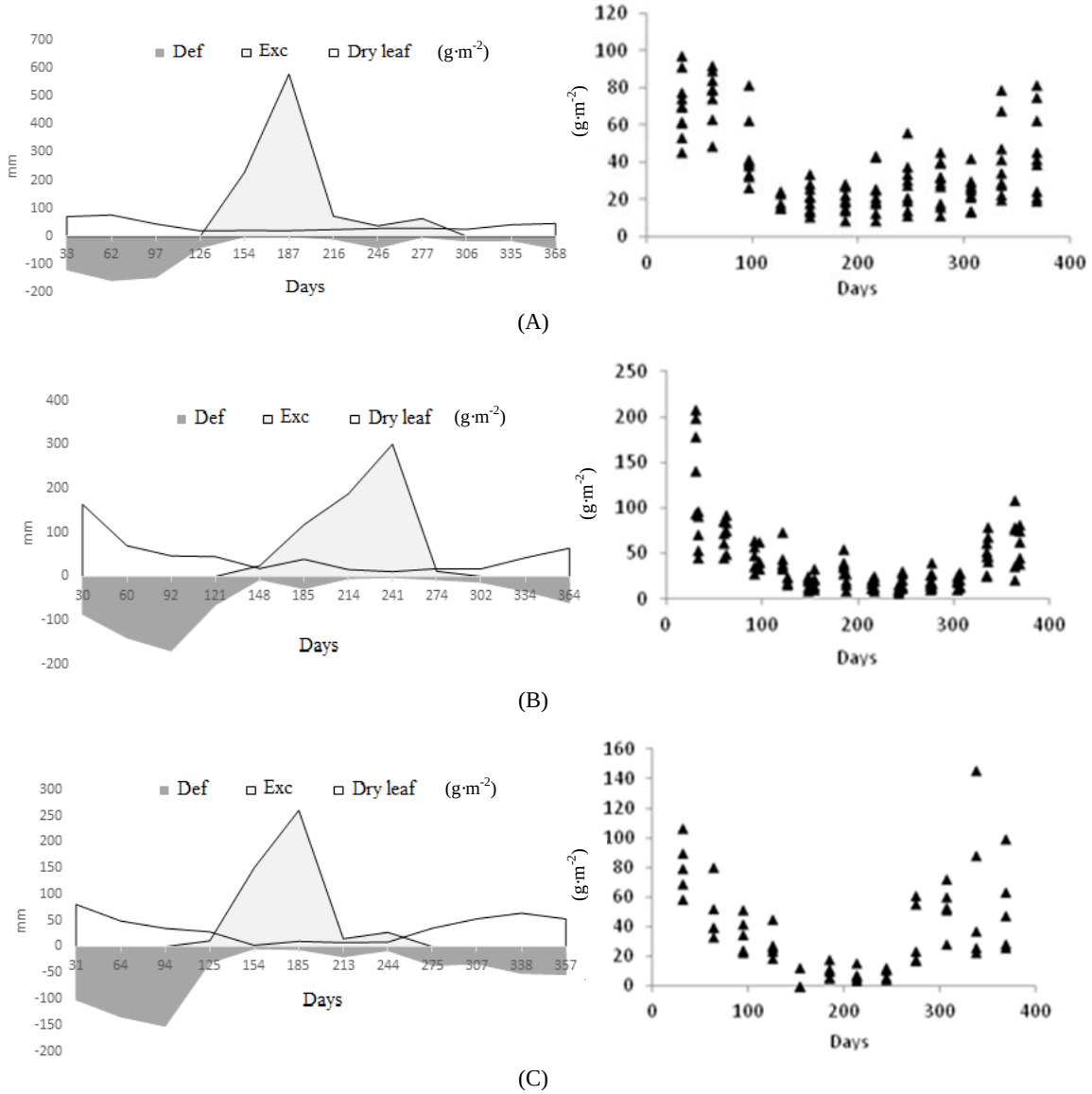

Fig. 2 Climatic water balance of Thornthwaite for 13/07/11-15/07/12 period (A), 28/07/14-28/07/15 (B) and 28/07/15-29/07/16 period (C) and deciduousness, in average leaf dry weight (g·m^{-2}) gotten by nets installed in parcels of 20 × 20 m inside the patch, distance of 80-100 meters from the edge, and observed values of leaf dry weight, to area 51, in period 15/08/11-15/07/12 (A), to area 81, in period 27/08/14-28/07/15 (B) and to area 61 in period 28/08/15-29/07/16 (C). Note 1: DEF (deficient) and EXC (surplus) water to each plant-available water capacity of the soil = 150 mm, establishing the same accumulation period between the water balance and the leaf dry weight. Note 2: Potential evapotranspiration considered until 18/07/16, the last day of conventional climatic station operation. The radiation data of the automatic station was not calibrated when it began operation.

The area 81 has predominance of the vertical plane of the vegetation edge in front of collect nets due to lower slope. That is, the surface area to leave litterfall is minor compared to area 51.

Referred to area 61, distance of nets collectors begins in three meters and the height of trees is lower (Table 1). Because of this, the litterfall is very lower in area 61.

The areas 81 and 61 are located on east, and the predominance of winds in the region is also from the east. Because of this, it reduces the amount of drift-contributing winds at direction of the patch to the

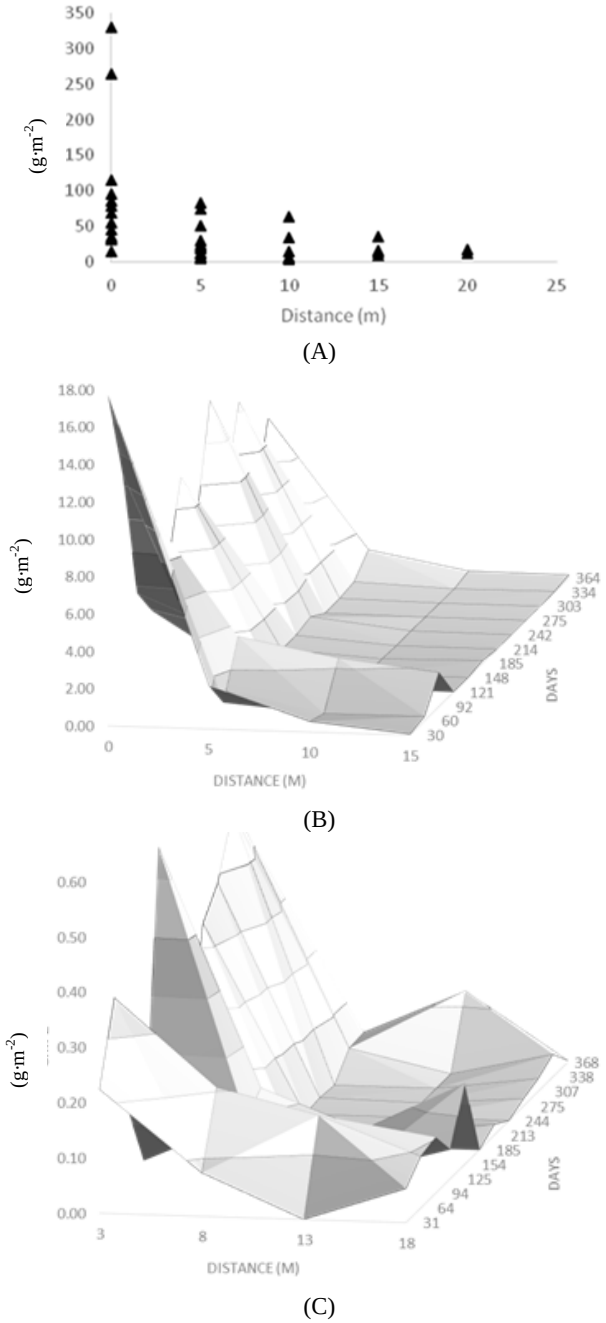

Fig. 3 Drift of litterfall (sum of branches, reproductive material and leafs) collected by distance in: (A) area 51 from period of 13/07/11 to 18/10/11 (95 days); (B) average values of the area 81; and (C) average values of the area 61, by periods.

adjacent area.

Table 3 shows the velocity wind frequencies and Table 4 shows the direction wind frequencies, for three periods. The factors (Fwp) to velocity wind and direction wind in each period were calculated by Eqs. (1)-(4).

In Fig. 4, authors can evaluate the estimates of model with wind and hydric balance. The area 51 has only one period with sums of components (br + rm + lf). The results shown in Fig. 4A correspond to the estimated values with and without the wind factor, without observed values.

In all areas and components of litterfall, estimates with model considering wind factor did not contribute enough to accuracy of results.

Authors supposed that it happened due to imprecision of wind. It is collected far 6-8 kilometers of areas and relief may interfere on direction and velocity.

In area 81, leaf deposition had the best estimate per period and yearly, followed by reproductive material. The estimate in area 61, three meters from edge distance per period, was the least accurate, including for leaf deposition, reflecting the annual distance estimate.

The amount of leaves deposited externally in the periods follows the same tendency into the patch, which does not occur for branches and reproductive material (flowers, fruits and seeds), because the water regime influences only the leaf drift.

In the comparison of the estimated and observed values, the branch component suffers less influence of winds due to its area/volume ratio. In addition, its fall has a predominant cause for the senescence in part of the plant, that is to say, the effect of the water deficit is not preponderant factor for fall of branches. The fall is also influenced by the increase of the weight by the absorption of the water by the wood, indicating that the rain can influence the fall of branches.

The reproductive material also showed large deviations between observed and estimated values, because the phenological phases of flowering and fruiting are not governed by winds and water regime only, and occur at different times among species. Thus, each site will produce propagules in different periods

Table 3 Tables of frequency at hour 12 for speed wind and factor per period (Fwp). (Hours 18 were omitted because they are analogous to those presented).

Sp. wind_12 h	1	2	3	4	5	6	7	8	9	10	11	12	Total
0	1				5	9	4	2	4	4	4	3	36
0.5	2	2	3	3	5	9	5	1	6	7	13	8	64
1	7	2	2	5	9	6		4	3	7	3	7	55
1.2						2	6	4					12
1.5	10	10	9	9	2			3	8	9	7	9	76
1.7						2	3	1					6
2.1	4	6	5	2	2	3		1		1	1	3	28
2.4							3	3					6
2.6	5	3	3	2	2				1	1		2	19
2.9							3	4					7
3.1	2		1	2		1		2	2		1	1	12
3.6	1	1	4	3	2	1	4	4	4				24
4.1	1	3	2	3			1		2				12
4.6		1	3					1	1				6
5.1		1	2										3
5.7			1		1								2
1 Total	33	29	35	29	28	33	29	30	31	29	29	33	368
Fwp	1.77	2.21	2.59	2.02	1.31	0.89	1.70	2.05	1.74	0.99	0.87	1.18	
0		1				1	1	2			1		6
0.5	4	2			4	2	4	1	3	5	9	5	39
1	4	4	2	8	2	9	6	11	11	5	8	4	74
1.5	5	2	5	7	4	14	7	6	7	4	6	14	81
2.1	7	4	5	7	6	4	6	4	5	8	4	3	63
2.6	4	4	4	1	5	3	3	2	2	1	2	1	32
3.1	2	2	2	5	3	2		1	4	1		1	23
3.6	1	1	5		3	1			1	1	1	2	16
4.1	2	4	3	1			1			3			14
4.6			5				1				1		7
5.1	1												1
5.7		2	1										3
6.2		3				1							4
7.2		1											1
2 Total	30	30	32	29	27	37	29	27	33	28	32	30	364
Fwp	2.06	3.01	2.99	1.91	2.06	1.71	1.64	1.38	1.66	1.85	1.35	1.56	
0			1			2		4		2			9
0.5		3		1	3	3	5	5	2	7	2	2	33
1	5	10	3	9	8	5	5	6	8	6	9	7	81
1.5	9	10	5	9	7	13	11	7	10	7	9	4	101
2.1	3	3	9	3	6	5	4	2	4	3	6	4	52
2.6	3	2	5	4	2		2	1	2	5	3	6	35
3.1	2	2	3	3	2	2	1	3	1		1	1	21
3.6	3	1	2	1	1	1		3	2	1	1	3	19
4.1	1	1	2						2	1			7
4.6	1											2	3
5.1	2											1	3
5.7	1			1									2
6.2		1											1
7.2	1												1
3 Total	31	33	30	31	29	31	28	31	31	32	31	30	368
Fwp	2.63	1.76	2.24	1.88	1.64	1.49	1.45	1.48	1.81	1.47	1.63	2.21	

Table 4 Tables of frequency at hour 12 for direction wind and factor per period (Fwp).

Dir. wind_12 h	1	2	3	4	5	6	7	8	9	10	11	12	Total
no wind	1				5	6	2	3	4	4	4	4	33
E	13	19	23	11	12	6	19	23	15	5	5	10	161
N	1	4	2	2	6	11	1	1	1	1	3	1	34
NE	2	1	4	6	1	5	1		2	1	1		24
NW	1			1	2	3	1						8
S	1		1	4				1	4	10	6	6	33
SE	11	5	3	5	2	2	5	2	3	5	7	7	57
SW			1						1	2	3	2	9
W	3		1						1	1		3	9
1 Total	33	29	35	29	28	33	29	30	31	29	29	33	368
Fwp	0.21	0.17	0.23	0.31	0.32	0.58	0.10	0.03	0.16	0.17	0.24	0.18	
no wind		1				1	1	2			1		6
E	16	18	20	13	9	19	15	12	16	9	12	15	174
N		1	1	1	4	3	3	4	1	2	1		21
NE	1	1	4	7	5	5	2	2		2		1	30
NW	1		1				1			1			4
S	3	2	1	4	2	4		2	6	10	6	4	44
SE	6	7	5	3	6	3	4	2	7	4	6	8	61
SW	1					2			2		1	1	7
W	2			1	1		3	3	1		5	1	17
2 Total	30	30	32	29	27	37	29	27	33	28	32	30	364
Fwp	0.13	0.07	0.19	0.31	0.37	0.22	0.31	0.33	0.06	0.18	0.19	0.07	
no wind			1			2		4		2			9
E	21	13	12	9	10	9	10	8	15	7	5	11	130
N		3	1	6	4	7	3	5	1	2	1	1	34
NE	1	2	8	7	3	4	5	1		2		1	34
NW					1				1		1	1	4
S	2	5	5		6	3	1	1	2	8	4	5	42
SE	7	8	3	8	3	4	8	11	11	8	10	10	91
SW				1	1			1		1	5	1	10
W		2			1	2	1		1	2	5		14
3 Total	31	33	30	31	29	31	28	31	31	32	31	30	368
Fwp	0.03	0.21	0.30	0.42	0.31	0.42	0.32	0.19	0.10	0.19	0.23	0.10	

Note: shadow directions contribute to collectors.

according to the floristic diversity, confirming that samples inside the patch are not representative to infer in the drift of the reproductive material.

Table 5 shows the litterfall quantities deposited in the reference periods within the patch (only leafs), at the border and by distance of the patch (sum of branches, reproductive material and leaves). Although the periods are different, there is no relevant variation regarding the water regime and the favorable directions and speed frequencies of the winds strongly affecting the deciduousness.

In order to obtain a model with equation of the behavior of litterfall deposition in one year, authors worked with annual average values by distance. Fig. 5 shows the curve adjusted in the logarithmic model (Eq. (7)) for litter deposition ($g \cdot m^{-2}$) versus the distance for the each period. The Eq. (8) of the area 51 with R^2 98.4%, and Eqs. (9) and (10) with R^2 100% to area 81 and 61 respectively, were different.

The content and reach depend of conditions, how structure of vegetation, position of the fragment and adjacent area and wind.

$$Y = a * exp(b * X) + c \quad (7)$$

$$d.w.(g.m^{-2}) = 190.64778193248 * exp(-0.154435144400618 * meters) + 0 \quad (8)$$

$$d.w.(\frac{g.m^{-2}}{year}) = 548.042819055106 * exp(-0.494151732272885 * meters) + 1.76845451404677 \quad (9)$$

$$d.w.\left(\frac{g.m^{-2}}{year}\right) = 426.670674190849 * exp(-0.628153630058945 * meters) + 0.30328368906145 \quad (10)$$

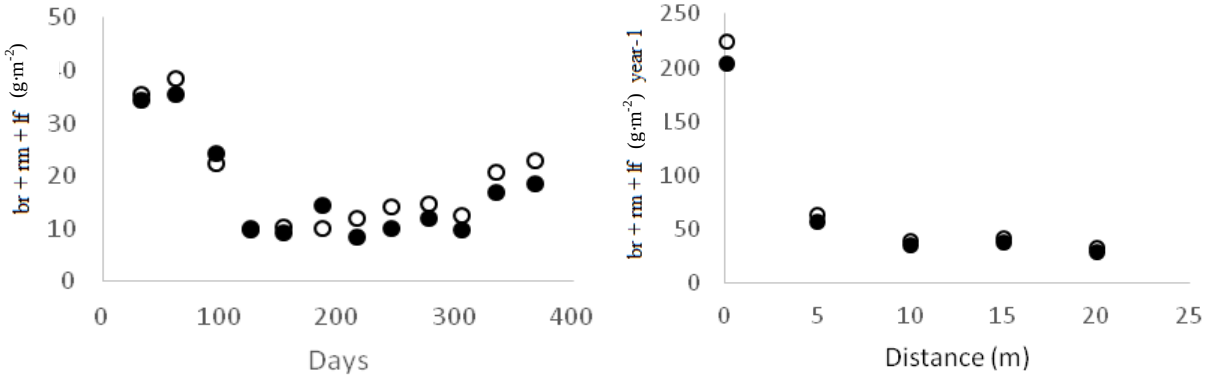

(A)

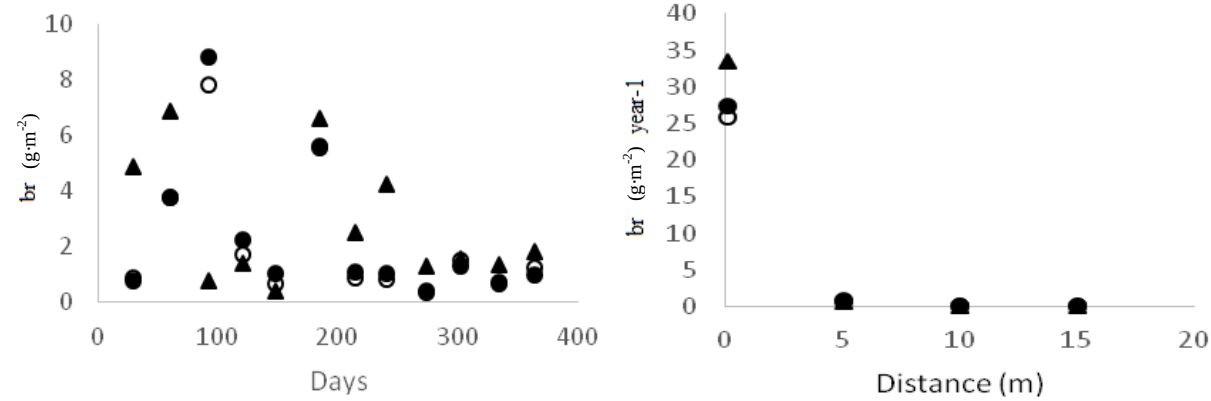

(B1)

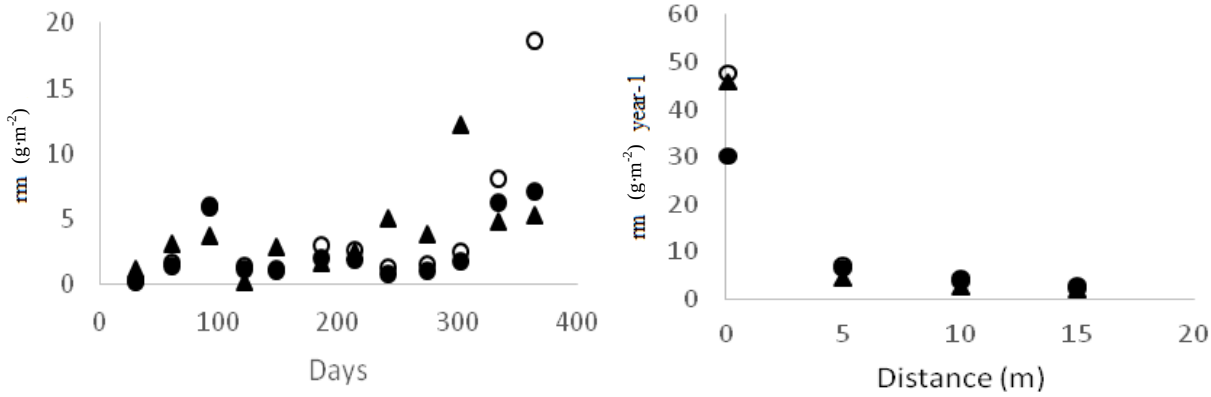

(B2)

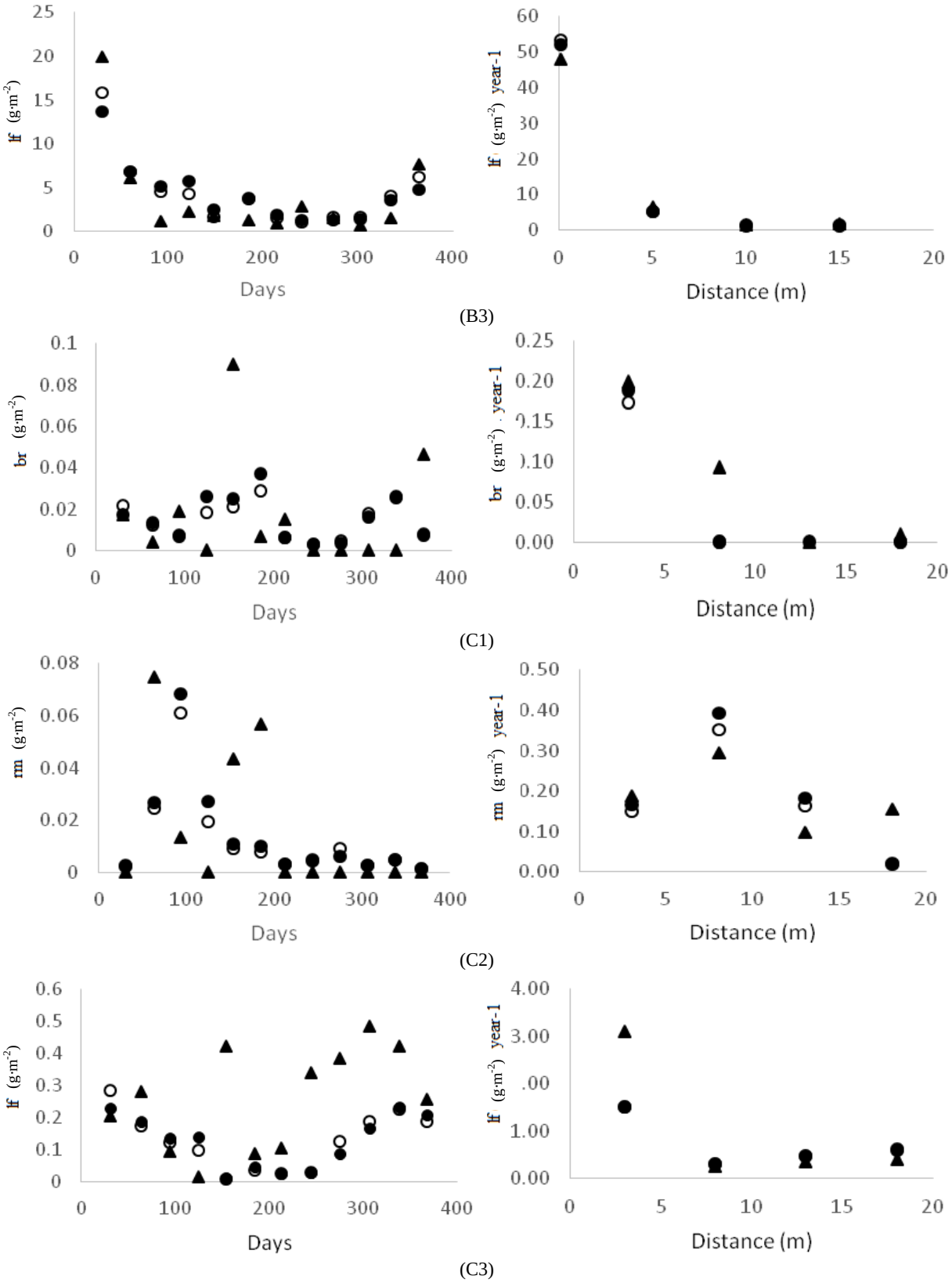

Fig. 4 Litterfall observed (▲), estimate (●), estimate less wind's model (○) on edge by periods (left graphs), and by distances in one year (right graphs), in which br: branch; rm: reproductive material; lf: leaf, to area 51 (A), area 81 (B) and area 61 (C).

Table 5 Litterfall deposition (branches, reproductive material and leaves) by distance, weighted average wind speed and favorable wind frequencies for 12 h and 18 h UTC, and water deficit for the reference periods.

	Period ref.	18/10/11*	27/08-28/10/14	28/08-30/10/15
		$g \cdot m^{-2}$		
Patch	lf	190.64	280.7	164.42
Edge	br + rm + lf	96.3	47.5	
3 m	br + rm + lf			0.71
5 m	br + rm + lf	27.1	6.62	
8 m	br + rm + lf			0.33
10 m	br + rm + lf	16.7	3.4	
13 m	br + rm + lf			0.28
15 m	br + rm + lf	17.8	2.7	
18 m	br + rm + lf			0.26
20 m	br + rm + lf	13.7	-	
Weighted average of wind speed ($m \cdot s^{-1}$)		0.57	0.62	0.52
Frequency of favorable winds		59 (N, NE, NW, SW, W)	47 (N, NE, NW, W)	59 (N, NE, NW, W)
Water deficit (mm)		-413.7	-395.29	-387.09

*The period is 95 days and it began on 13/07/11.

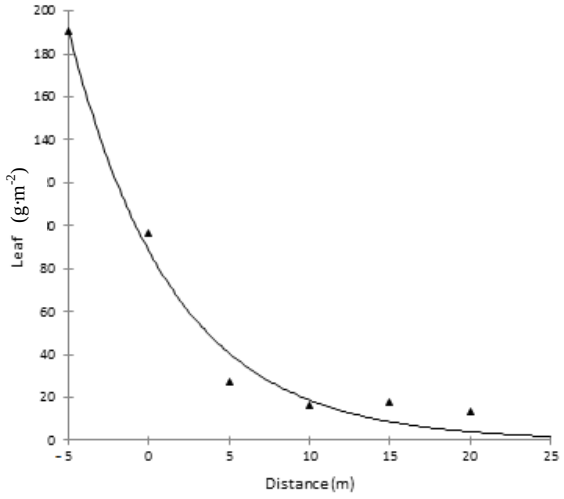

(A)

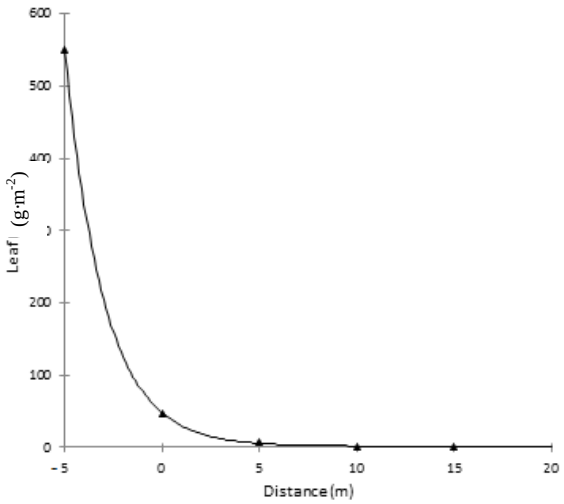

(B)

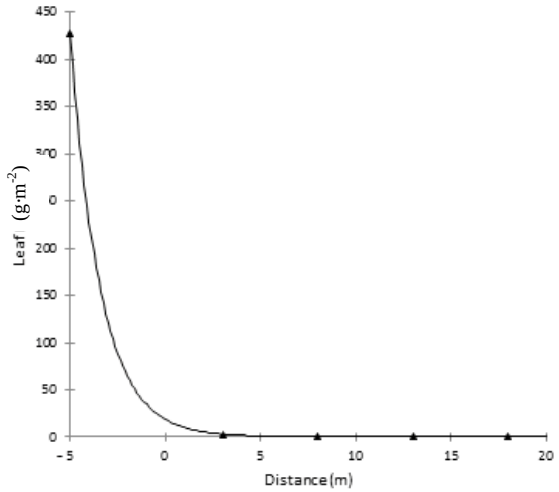

(C)

Fig. 5 Dry weight average of litterfall (d.w.) as function to the distance of the patch for the collection (A): period 15/07/11 to 18/10/11 (g/m^2), for (B): the period of 27/08/14 to 28/07/15 and (C): period 28/08/15 to 29/07/16 (g/m^2/year).

Then, the drift of nutrients from forests to adjacent areas is function of distance from the edges, and the wind conditions, topographical surfaces and structure of vegetation will influence. At the areas 51, 81 and 61, the quantity of nutrients deposited by distance in one year can be estimated. This was done to nutrients of the leaves. The leaf analysis of macro and micronutrients from leaves collected within the patch is presented in Table 6, and the amount of nutrients

deposited in kg/ha/year into the forest, as it moves away from the edge, is given in Table 7.

Maize is reference crop in Brazil, common in family farming and broad-spectrum in agricultural activity. It is used data from export of nutrients at maize harvest, according to their productivity [30] (Table 8), for calculating the percentage of nutrients that the forest can offer in the replacement of these nutrients, disregarding factors affecting the mineralization of organic matter.

Table 6 Quantity of average nutrients of the litter leaves to rain and dry periods. Nitrogen (N) is not analyzed in dry period.

				N	P	K	Ca	Mg	Zn	Fe	Mn	Cu
Season	Area	Plot	Net	----------dag/kg (%)----------					----------mg/kg (ppm)----------			
rain	51	1	1	1.48	0.08	0.81	2.82	0.36	22.7	322.3	51.6	12.8
			2	1.81	0.09	1.08	2.81	0.46	36.0	469.6	90.0	11.1
			3	0.96	0.07	0.60	2.31	0.31	40.3	324.8	115.4	4.9
			4	1.73	0.08	0.81	2.30	0.30	23.9	407.2	143.9	13.5
			5	1.65	0.08	0.67	2.56	0.31	27.9	389.5	82.1	11.9
		2	1	1.34	0.09	0.90		0.33	28.3	376.7	78.6	6.0
			2	1.27	0.09	0.75	1.87	0.21	29.8	360.4	67.5	9.0
			3	1.13	0.10	0.64	1.86	0.21	25.7	369.8	119.0	5.9
			4	1.19	0.15	0.66	1.96	0.21	24.4	334.1	79.5	7.0
			5	1.19	0.11	0.69	2.03	0.21	34.8	357.5	79.5	6.5
	61	3	1	1.14	0.11	0.94	1.67	0.28	28.1	274.8	185.7	6.9
			2	1.04	0.18	0.70	1.63	0.23	26.5	317.4	199.9	4.3
			3	1.05	0.20	0.82	1.92	0.26	20.5	291.4	325.1	6.5
			4	1.19	0.16	1.02	2.52	0.40	26.9	313.4	161.6	8.8
			5	1.24	0.17	1.14	2.38	0.31	27.6	369.4	140.9	7.6
	81	1	1	1.36	0.06	0.84	1.83	0.38	28.6	247.8	351.2	7.4
			2	1.14	0.08	0.85	1.61	0.26	27.8	157.8	298.8	7.7
			3	1.24	0.06	0.66	2.01	0.28	21.3	237.5	297.6	6.9
			4	1.13	0.06	0.57	1.88	0.27	25.1	286.3	318.2	7.8
			5	1.19	0.06	0.60	1.48	0.23	27.0	237.4	369.2	6.3
dry	51	1	1		0.14	0.84	2.81	0.36	27.88	377.09	106.05	16.66
			2		0.16	0.86	2.69	0.39	31.26	350.86	129.69	9.84
			3		0.11	0.53	2.18	0.34	29.12	497.30	214.33	10.85
			4		0.10	0.72	2.34	0.35	25.40	668.71	337.25	14.26
			5		0.13	0.72	3.11	0.37	30.34	632.95	132.10	14.86
		2	1		0.13	0.65	3.27	0.35	23.59	500.48	196.91	8.50
			2		0.21	0.88	2.06	0.32	47.37	804.16	103.89	22.89
			3		0.18	0.69	2.18	0.33	35.37	553.53	189.49	12.59
			4		0.18	0.62	2.53	0.31	31.68	621.45	240.64	11.42
			5		0.19	0.90	2.69	0.30	37.45	765.79	146.10	14.62
	61	3	1		0.14	0.71	2.34	0.35	41.42	465.73	362.76	10.36
			2		0.22	0.66	1.88	0.34	38.32	399.24	297.13	9.93
			3		0.18	0.77	2.07	0.29	25.66	538.18	300.59	12.77
			4		0.15	0.60	2.18	0.33	28.44	373.50	192.84	11.39
			5		0.17	0.86	2.29	0.42	40.89	558.86	235.04	12.23
	81	1	1		0.11	0.85	2.36	0.45	25.27	442.93	298.77	10.79
			2		0.09	0.76	2.21	0.43	23.15	302.70	283.47	10.01
			3		0.10	0.66	2.64	0.43	27.61	252.55	278.90	9.72
			4		0.09	0.46	2.50	0.36	26.01	299.77	260.01	11.43
			5		0.14	1.04	3.48	0.65	25.63	419.43	281.05	10.35

Table 7 Nutrients quantity (kg/ha/year) deposited by leaves as function of distance of patch.

Area	Position	N	P	K	Ca	Mg	Zn	Fe	Mn	Cu
51	Patch	55.31	5.31	29.93	95.27	12.98	0.12	2.00	0.60	0.05
	edge	25.56	2.45	13.83	44.01	6.00	0.06	0.93	0.28	0.02
	5 m	11.81	1.13	6.39	20.33	2.77	0.03	0.43	0.13	0.01
	10 m	5.45	0.52	2.95	9.39	1.28	0.01	0.20	0.06	0.00
	15 m	2.52	0.24	1.36	4.34	0.59	0.01	0.09	0.03	0.00
	20 m	1.16	0.11	0.63	2.01	0.27	0.00	0.04	0.01	0.00
81	Patch	66.14	5.04	40.91	130.49	22.71	0.14	1.68	1.62	0.05
	edge	5.59	0.43	3.46	11.03	1.92	0.01	0.14	0.14	0.00
	5 m	0.47	0.04	0.29	0.93	0.16	0.00	0.01	0.01	0.00
	10 m	0.04	0.00	0.02	0.08	0.01	0.00	0.00	0.00	0.00
	15 m	0.00	0.00	0.00	0.01	0.00	0.00	0.00	0.00	0.00
61	Patch	48.30	7.10	32.12	90.29	13.96	0.14	1.82	1.09	0.04
	3 m	0.32	0.05	0.21	0.59	0.09	0.00	0.01	0.01	0.00
	8 m	0.01	0.00	0.01	0.03	0.00	0.00	0.00	0.00	0.00
	13 m	0.00	0.00	0.00	0.00	0.00	0.00	0.00	0.00	0.00
	18 m	0.00	0.00	0.00	0.00	0.00	0.00	0.00	0.00	0.00

Table 8 Nutrition requirements (kg/ha) of maize crop for productivity of 3.65 t/ha [30], and percent of reposition of macro and micronutrients offered by forest patches.

Area		kg/ha								
		N	P	K	Ca	Mg	Zn	Fe	Mn	Cu
		77	9	83	10	10	0.16	0.84	0.14	0.04
	Dist.(m)	% provided by leaves of litterfall								
51	Patch	71.84	59.00	36.06	952.68	129.80	76.87	239.80	443.88	107.27
	edge	33.19	27.26	16.66	440.14	59.97	35.51	110.79	205.08	49.56
	5 m	15.33	12.59	7.70	203.35	27.70	16.41	51.19	94.75	22.90
	10 m	7.08	5.82	3.56	93.95	12.80	7.58	23.65	43.77	10.58
	15 m	3.27	2.69	1.64	43.41	5.91	3.50	10.93	20.22	4.89
	20 m	1.51	1.24	0.76	20.05	2.73	1.62	5.05	9.34	2.26
81	Patch	85.90	56.02	49.29	1,304.94	227.06	88.64	201.35	1,200.02	118.17
	edge	7.26	4.74	4.17	110.29	19.19	7.49	17.02	101.43	9.99
	5 m	0.61	0.40	0.35	9.32	1.62	0.63	1.44	8.57	0.84
	10 m	0.05	0.03	0.03	0.79	0.14	0.05	0.12	0.72	0.07
	15 m	0.00	0.00	0.00	0.07	0.01	0.00	0.00	0.00	0.00
61	Patch	62.73	78.94	38.69	902.89	139.63	85.18	217.39	805.70	101.64
	3 m	0.41	0.52	0.25	5.93	0.92	0.56	1.43	5.29	0.67
	8 m	0.02	0.02	0.01	0.26	0.04	0.02	0.06	0.23	0.03
	13 m	0.00	0.00	0.00	0.01	0.00	0.00	0.00	0.01	0.00
	18 m	0.00	0.00	0.00	0.00	0.00	0.00	0.00	0.00	0.00

The results show that the contribution to the soil fertility maintenance in the surroundings of forest patch can vary a lot. The replacement of Ca by leaves deposition reaches 43% at a distance of 15 meters in area 51, but to areas 81 and 61, the amount of nutrients is already very lower in 3 meters due to lower drift of leaves in these places.

The great variation of the nutrient deposition by the distance between the areas shows that the contribution of vegetable material by means of drift to areas of the forest surroundings has a great influence of the vegetation structure, not only the water balance,

topographical configuration and winds.

Even if the annual supply of nutrients by air has small magnitude, in long periods of accumulation, the amount can be considered a benefit for agriculture, especially with low input use, when chemical fertilizers are not applied. With a multiplicative annual effect of the deposited material, one can have the dimension of how much the forests contribute to the improvement of the quality of the soil for the surrounding areas.

The nutritional contribution of forest ecosystems for these areas is an ecosystem service [21]. It is likely that the major importance of this kind of supply of nutrients occurs in mountain agriculture, in wavy relief, with forest in the tops and pastures and fields on the slopes. And it has many small crops and grassland in farms vicinity of environmental reserves. In all these environments, this kind of deposition of organic matter can be increased by the mobility of nutrients through runoff and leaching upstream, not measured in this work.

4. Conclusion

Neighboring areas of forest ecosystem studied receive contribution of litterfall and their nutrients contained in the organic matter through drift.

The variation of drift of litterfall to adjacent areas is large. It depends of structure of vegetation, direction of wind and topography of area. The estimates with model considering wind factor did not contribute enough to accuracy of results.

It was confirmed that model estimated the leaf drift by distance with good precision.

Acknowledgments

Thanks to Project CNPq 487727/2013-4—Agroecological production of the field to city, performance of the Guayi Agroecology Group as CVT (Technological Vocational Center) in Agroecology and Organic Production in Minas Gerais State and Project MP6 06.14.07.006.00.02.008—Agroecological Transition. Authors thank to Vinicius Leal and Iago Ferreira who helped in installation and measurements of data, and to Dra Leila Ferraz, Coordinator of the CNPq Project by support for this research.

References

[1] Andrade, A. G., Tavares, S. D. L., and Coutinho, H. D. C. 2003. “Contribuição da Serapilheira para Recuperação de Areas Degradadas e para Manutenção da Sustentabilidade de Sistemas Agroecológicos.” *Informe Agropecuário* 24 (220): 55-63. (in Portuguese)

[2] Menezes, C. E. G., Pereira, M. G., Fernandes Correia, M. E., Cunha dos Anjos, L. H., Ribeiro Paula, R., and de Souza, M. E. 2010. “Aporte e Decomposição da Serapilheira e Produção de Biomassa Radicular em Florestas com Diferentes Estágios Sucessionais em Pinheiral, RJ.” *Ciência Florestal* 20 (3): 439-52. (in Portuguese)

[3] Ewel, J. J. 1976. “Litter Fall and Leaf Decomposition in a Tropical Forest Succession in Eastern Guatemala.” *The Journal of Ecology* 64: 293-308.

[4] Nadelhoffer, K. J., and Blair, J. M. 1999. “Measuring Decomposition, Nutrient Turnover, and Stores in Plant Litter.” *Standard Soil Methods for Long-Term Ecological Research*: 202.

[5] Arato, H. G., Martins, S. V., and Ferrari, S. H. D. S. 2003. “Produção e Decomposição de Serapilheira em um Sistema Agroflorestal Implantado para Recuperação de Area Degradada em Viçosa-MG.” *Revista Árvore* 27 (5): 715-21. (in Portuguese)

[6] Spain, A. V. 1984. “Litterfall and the Standing Crop of Litter in Three Tropical Australian Rainforests.” *The Journal of Ecology* 72: 947-61. doi: 10.2307/2259543.

[7] Gomes, J. M., Pereira, M. G., Piña-Rodrigues, F., Pereira, G. H., Gondim, F. R., and da Silva, E. M. 2010. “Aporte de Serapilheira e de Nutrientes em Fragmentos Florestais da Mata Atlântica, RJ.” *Revista Brasileira de Ciências Agrárias* 5 (3): 383-91. (in Portuguese). doi: 10.5039/agraria.v5i3a552.

[8] Munari Vogel, H. L., Schumacher, M. V., Trüby, P., and Vuaden, E. 2007. “Avaliação da Devolução de Serapilheira em uma Floresta Estacional Decidual em Itaara, RS, Brasil.” *Ciência Florestal* 17 (3): 187-96. (in Portuguese)

[9] Maman, A. P., Silva, C. D., Sguarezi, E. M., and Bleich, M. E. 2007. “Produção e Acúmulo de Serapilheira e Decomposição Foliar em Mata de Galeria e Cerradão no Sudoeste de Mato Grosso.” *Revista de Ciências Agro-Ambientais* 5 (1): 71-84. (in Portuguese)

[10] König, F. G., Brun, E. J., Schumacher, M. V., and Longhi, S. J. 2002. "Devolução de Nutrientes via Serapilheira em um Fragmento de Floresta Estacional Decidual no Município de Santa Maria, RS." *Brasil Florestal* 74: 45-52. (in Portuguese). doi: 10.1590/S0100-67622002000400005.

[11] da Cunha, G. C., Grendene, L. A., Durlo, M. A., and Bressan, D. A. 1999. "Dinâmica Nutricional em Floresta Estacional Decidual com ênfase aos Minerais Provenientes da Deposição da Serapilheira." *Ciência Florestal* 3 (1): 35-64. (in Portuguese)

[12] da Silva Santana, J. A., and Silva Souto, J. 2011. "Produção de Serapilheira na Caatinga da Região Semiárida do Rio Grande do Norte, Brasil." *IDESIA* 29 (2): 87-94. (in Portuguese). doi: 10.4067/ S0718-34292011000200011.

[13] Costa, T. C. C., Viana, J. H. M., and Ribeiro, J. L. 2014. "Semideciduous Seasonal Forest Production of Leaves and Deciduousness in Function of the Water Balance, LAI and NDVI." *International Journal of Ecology*: 1-15. doi: 10.1155/2014/923027.

[14] Giácomo, R. G., Pereira, M. G., and Machado, D. L. 2012. "Aporte e Decomposição de Serapilheira em Areas de Cerradão e Mata Mesofítica na Estação Ecológica de Pirapitinga-MG." *Ciência Florestal* 22 (4): 669-80. (in Portuguese). doi: 10.5902/198050987549.

[15] Silva, C. D., Lobo, F. D. A., Bleich, M. E., and Sanches, L. 2009. "Contribuição de Folhas na Formação da Serapilheira e no Retorno de Nutrientes em Floresta de Transição no Norte de Mato Grosso." *Acta Amazonica* 39 (3): 591-600. (in Portuguese)

[16] Silva, C. J. D., Sanches, L., Bleich, M. E., Lobo, F. D. A., and Nogueira, J. D. S. 2007. "Produção de Serrapilheira no Cerrado e Floresta de Transição Amazônia-Cerrado do Centro-Oeste Brasileiro." *Acta Amazônica* 37 (4): 543-8. (in Portuguese). doi: 10.1590/S0044-59672007000400009.

[17] Vital, A. R. T., Guerrini, I. A., Franken, W. K., and Fonseca, R. C. B. 2004. "Produção de Serapilheira e Ciclagem de Nutrientes de uma Floresta Estacional Semidecidual em Zona Ripária." *Revista Árvore* 28 (6): 793-800. (in Portuguese). doi: 10.1590/S0100-67622004000600004.

[18] Filho Figueiredo, A., Moraes Ferreira, G., Schaaf Budant, L., and de Figueiredo, D. J. 2003. "Avaliação Estacional da Deposição de Serapilheira em uma Floresta Ombrófila Mista Localizada no sul do Estado do Paraná." *Ciência Florestal* 13 (1): 11-8. (in Portuguese)

[19] Poggiani, F., and Schumacher, M. V. 2000. "Ciclagem de Nutrientes em Florestas Nativas." *Nutrição e fertilização florestal. Piracicaba: IPEF*: 427. (in Portuguese)

[20] Ferreira, C. D. 2011. "Deposição, Acúmulo e Decomposição de Serapilheira em Area de Caatingapreservada [monograph]." Centro de Saúde e Tecnologia Rural, Universidade Federal da Paraíba. Campina Grande. (in Portuguese)

[21] Costa, T. C. C., and Miranda, G. A. 2014. "Nutritional Contribution of Litterfall for a Surrounding Forest Area According to the Distance of a Forest Fragment." *Journal of Environment and Ecology* 5 (2): 144-58.

[22] Losey, J. E., and Vaughan, M. 2006. "The Economic Value of Ecological Services Provided by Insects." *Bioscience* 56 (4): 311-23.

[23] De Marco, P., and Coelho, F. M. 2004. "Services Performed by the Ecosystem: Forest Remnants Influence Agricultural Cultures' Pollination and Production." *Biodiversity and Conservation* 13 (7): 1245-55.

[24] Zhang, W., and Swinton, S. M. 2009. "Incorporating Natural Enemies in an Economic Threshold for Dynamically Optimal Pest Management." *Ecological Modelling* 220 (9): 1315-24. doi: 10.1016/j.ecolmodel.2009.01.027.

[25] Costanza, R., d'Arge, R., De-Groot, R., Farber, S., Grasso, M., Hannon, B., et al. 1997. "The Value of the World's Ecosystem Services and Natural Capital." *Nature* 387 (6630): 253-60.

[26] Duncan, D. H., Dorrough, J., White, M., and Moxham, C. 2008. "Blowing in the Wind? Nutrient Enrichment of Remnant Woodlands in an Agricultural Landscape." *Landscape Ecology* 23 (1): 107-19. doi10.1007/s10980-007-9160-0.

[27] Allen, R. G., Pereira, L. S., Raes, D., and Smith, M. 1998. "Crop Evapotranspiration-Guidelines for Computing Crop Water Requirements-FAO Irrigation and Drainage Paper 56." *FAO, Rome* 300 (9): D05109.

[28] Angelocci, L. R., Sentelhas, P. C., and Pereira, A. R. 2002. "Agrometeorologia: Fundamentos e Aplicações Práticas." *Guairá: Agropecuária.* (in Portuguese)

[29] Costa, T. C. C., Silva, A. F., Oliveira, L. M. T. D., and Viana, J. H. M. 2015. "Probabilistic Classification of Tree and Shrub Vegetation on Phytogeographic System." *Journal of Environmental Science and Engineering B* 4 (6): 315-30.

[30] Cruz, J. C., Karam, D., Monteiro, M. A. R., and Magalhães, P. C. 2008. *A Cultura do Milho*. Sete Lagoas, Brazil: Embrapa Milho e Sorgo. (in Portuguese)

Journal of Environmental Science and Engineering A 6 (2017) 363-369
doi:10.17265/2162-5298/2017.07.004

Vegetative Habitus and Fruit Production of Self-rooted Cherry Cultivar 'Hedelfingen' Wild Type and Somaclonal Grafted on 'Gisela 6' and 'Colt' Rootstock

Piagnani Maria Claudia and Chiozzotto Remo

Department of Agricultural and Environmental Sciences, University of Milan, Milano 20133, Italy

Abstract: The study considers the morphological and physiological behaviour of self-rooted sweet cherry CV (Cultivar) 'Hedelfinger' wild type (H) and somaclonal (HS) grafted on 'Gisela 6' and 'Colt' rootstock. The somaclonal showed reduced vegetative vigour without any variation of the natural tree's architecture. The rootstock 'Gisela 6' caused change in genotype habitus inducing a spreading shape, while 'Colt' increased trunk diameter and height. Fruit quality and size were not affected by genotype nor rootstock. 'Gisela 6', from these preliminary data, had proved the most suitable rootstock for both genotypes since it reduced the tree size and vigor and induced early bearing and the production of a greater number of fruiting spurs.

Key words: Cherry CV 'Hedelfingen', growth habit, self-rooted somaclonal, 'Gisela 6', 'Colt', rootstock.

1. Introduction

Genetic variability occurring in plant tissue culture may have novel agronomic traits that can not be achieved by conventional breeding. Effect of root type and clone of 'Schattennmorelle' sour cherry upon growth and productivity was studied [1]. A lower vigor was significantly manifested by reduced increase of trunk, compared with the tree rootstocks. Self-rooted trees gave a lower yield per tree; however, their cropping efficiency index was 23-28% higher than that of trees grown on seedling rootstocks. Tissue culture generates a wide range of genetic variation in plant species, which can be incorporated in plant breeding programmers [1]. By *in vitro* selection, mutants with useful agronomic traits e.g. salt or drought tolerance or disease resistance, can be isolated in a short duration [2]. Moreover, root genotype affects many physiological parameters as water relations, leaf gas exchange and chlorophyll a fluorescence pigments, metabolites and fruit quality indices of cherry cultivar growing on rootstock with differing size-controlling potentials [3]. Other important agronomic traits of rootstock include compatibility, good tolerance to root hypoxia, water use efficiency, aptitude to uptake soil nutrients, tolerance to soil or water salinity, resistance/tolerance to pests and diseases, such as nematodes, soil-borne fungi, crown gall, bacterial canker and several virus, viroids and phytoplasms [4].

The lease of somaclonal as commercial cultivars has only sporadically included woody temperate fruit species. Somaclonal variation has provided a new and alternative tool to the breeders for obtaining genetic variability relatively rapidly and without sophisticated technology in horticultural crops, which are either difficult to breed or have narrow genetic base [5]. Somaclonal variant, named HS, regenerated from *Prunus avium* 'Hedelfingen' leaf tissue, exhibited different pattern of growth and development and reduced vigor respect to wild type under different light qualities of *in vitro* and early ex vitro conditions [6, 7]. The HS, somaclonal fruits quality at early unripe (green) and full ripe (dark red) stages did not show main biochemical differences respect to wild type fruit

Corresponding author: Piagnani Maria Claudia, Ph.D., research field: plant *in vitro* culture.

[8]. The proteomic analysis identified 39 proteins differentially accumulated between H and HS fruits at the two ripening stages, embracing enzymes involved in several pathways, such as carbon metabolism, cell wall modification, stress response and secondary metabolism. The evaluation of fruit phenolic composition by mass spectrometry showed that HS sweet cherries have higher levels of procyanidin, flavonol and anthocyanin compounds [9].

Tree size reduction is one of the most relevant aspects of cherry plant cultivated in field. New scion somaclonal HS could also represent a genetic source for breeding programs. The present research pursues the characterization of the somaclonal HS grafted on 'Gisela 6' (G6) and 'Colt' (Ct) in orchard system after 5 years of cultivation.

2. Material and Methods

2.1 Cultivation System

Self-rooted cherry trees CV 'Hedelfingen' (H) and its somaclone HS were transplanted in May 2005 in the "Fondazione Minoprio" Orchard (Vertemate-Como, Italy) and they blossomed in March 2011. Cherry trees CV 'Hedelfingen' and somaclonal HS, grafted on 'Gisela 6' (G6) and 'Colt' (Ct) rootstocks in October 2007 at the Department of Agricultural Science of University of Bologna, were transplanted in February 2008 in the "F. Dotti" Experimental Farm of University of Milan, and they blossomed on 16th April 2010.

2.2 Plant Vigor

Plants surveys were carried out on May/June of the first blossoming year (2010/2011). The data were detected after dividing the canopy into three segments: basal, middle and apical as described in Piagnani, M. C., et al. [6]. The following parameters were measured: collar stem diameter at 20 cm, plant height, long branch of one year, internodes length, leaves (width, length, area and petiole length), insertion angles and extension, n°/buds/fruit and wood in the branches of two and three years.

On self-rooted trees, 20 representative branches from wild type cherry CV 'Hedelfingen' and HS were chosen, while on grafted ones, the measurements were performed on all the branches present on the tree.

2.3 Fruit Quality

Fruit sugar content was assessed by digital refractometer (Atago, Tokyo, Japan) and acidity by titration with NaOH 01 N (Compact-S Titrator; Crison, Modena, Italy) on cherry juice and skin color by Minolta CR300. Reflectance colorimeter (Chromameter CR-300; Minolta, Osaka, Japan) within two ripening classes, measuring a* and b* minimum, maximum and average value of the L*a*b* CIELAB scale, represented the change in color green to red (a* value) and blue to yellow (b* value).

2.4 Statistical Analysis

The data processing was performed by ANOVA (Analysis of Variance) using SPSS.18 software (SPSS Inc., Chicago, IL, USA). Significant differences were calculated by Tukey's mean test.

Differences at $p \leq 0.05$ were considered as significant.

3. Results and Discussion

3.1 Plant Vigor

Self-rooted somaclonal (HS) has shown, respect wild-type (H), a reduced trunk diameter and height and longer shoots and internode, while branch angles do not show any difference (Table 1A). The rootstock has not influenced the HS development except for the increase of shoot length by 'Gisela 6' rootstock. On the contrary, 'Hedelfingen' grafted on 'Colt' has increased trunk diameter and tree height, but has significantly reduced internode length (Table 1B). Tree habitus has not modified in self-rooted genotypes, while 'Gisela 6' rootstock has induced a wider shape than 'Colt' increasing both crotch and extension angles, since the average angle of insertion and

extension has been rated 65° and 48° for 'Colt' and 81° and 73° for 'G6' (Table 1B).

Size leaf measures have taken into account: lamina length, lamina width and leaf area; width/length and petiole length. Self-rooted HS has shown shorter leaves and petiole (Table 2A) and the interaction of genotype and rootstock has been manifested by the reduction of leaf width in H/'G6' combination. HS has shown larger leaves in self-rooted plants and in both the rootstock combination. Rootstock 'G6', in general, leads to a more elongated shape of the leaf, while the combination 'H' on 'Ct' gives the less elongated. The combination HS/'G6' gave the longer petiole, while in self-rooted, the somaclonal petiole was shorter than the wild type (Table 2B).

3.2 Fruit Quality

Skin color, determined by CIELAB scale, did not show differences in fruit of the two genotypes within each ripening class (Table 3).

Fruit sugar content (SSC (Soluble Solid Content)) and acidity were not different within the three different ripening classes and the two genotypes (Table 4).

Rootstock 'Gisela 6' induced a significant increase in the number of flowers per inflorescence and this effect was higher in the Somaclone HS instead wild type H (Table 5).

Self-rooted cherry trees were transplanted on May 10th, 2005 after four years on May 8th, 2009. H (wild type) was very vigorous while HS (somaclone) was very small (Fig. 1).

Both the cultivars, WT (Wild Type) and HS grafted on 'Gisela', blossomed at the second year (Fig. 2). Only 25% of the trees grafted on 'Colt' blossomed in the second year and 60% of them did it in the third season.

Cherry fruit at the first ripeness stage were collected on May 25th, 2013 (H = WT; HS = somaclonal) (Fig. 3) and on May 30th, 2013 for the second ripeness stage (Fig. 4).

The average cherry production was respectively 785 g for the 'Wild Type' and 1,222 g for the somaclonal variant; these differences were not statistically significant.

Table 1 Trunk diameter, height, one year shoot and internode length, crotch (α°) and extension (β°) angle. (A) self-rooted (§n = 5) and (B) grafted trees (Xn = 8): genotype and rootstock interaction.

Genotype		Trunk diameter (cm)	Height (cm)	One year shoot (cm)	Internode length (cm)	Crotch (α°)	Extension (β°)
(A)	H	10.8§	341.6§	46.9	3.9	65.3	65.7
	HS	6.2*	243.5*	54.1*	4.4*	67.8	68.8
(B)	H/'G6'	3.0 a	165.4 a	33.3 ab	2.8 b	78.8	71.3
	H/'Ct'	4.5 b	233.7 c	28.5 a	2.3 a	63.7	45.6
	HS/'G6'	3.9 a	183.3 a	36.6 b	2.9 b	83.9	75.9
	HS/'Ct'	3.3 a	181.8 a	27.8 a	2.7 b	67.7	50.5

Note: * and different letters represent significant differences for P > 0.05.

Table 2 Leaf measurements: lamina length, lamina width and leaf area, width/length and petiole length. (A) self-rooted and (B) grafted trees: genotype and rootstock interaction.

Genotype		Lamina length (cm)	Lamina width (cm)	Lamina area (cm^2)	Lamina width/length	Petiole length (cm)
(A)	H	14.9	7.3	109.5	0.49	3.2
	HS	14.4*	7.4	107.2	0.52**	2.8*
(B)	H/'G6'	12.3 a	5.3 a	66.0 ab	0.43 a	3.7 a
	H/'Ct'	11.1 a	5.6 b	63.6 a	0.51 c	3.7 a
	HS/'G6'	13.5 a	5.8 b	79.5 c	0.43 a	4.5 b
	HS/'Ct'	12.4 a	5.7 b	71.2 b	0.47 b	3.3 a

Note: * and different letters represent significant differences for P > 0.05.

Table 3 Fruit skin color as assessed by Minolta for wild type (H) and somaclonal (HS) within the two ripening classes (a* and b* minimum, maximum and average value of the L*a*b* Minolta CIELAB scale).

CIELAB	Genotype	Date	Ripening class	Number	Min	Max	Average	Standard deviation
a*	H	May 25th	1	125	22.1	44.0	35.0	4.2
a*	H	May 30th	2	124	5.7	30.7	18.0	5.8
a*	HS	May 25th	1	67	19.5	44.3	34.4	5.7
a*	HS	May 30th	2	58	6.1	28.2	16.0	4.8
b*	H	May 25th	1	124	2.5	18.8	11.3	3.0
b*	H	May 30th	2	124	0.9	14.5	3.9	2.6
b*	HS	May 25th	1	67	1.1	18.8	11. 0	4.2
b*	HS	May 30th	2	58	0.9	15.8	3.3	2.6

Table 4 Fruit qualityfor wild type (H) and somaclone (HS) within the two ripening classes (ns = not significant).

Genotype	Date	SSC (Brix°)	Acidity (meq)
H	25/05	20.6 ns	--
	30/05	20.4 ns	11.2 ns
	6/06	16.9 ns	8.5 ns
HS	25/05	21.4 ns	--
	30/05	19.7 ns	11.3 ns
	6/06	17.1 ns	8.3 ns

Table 5 Flowers per inflorescence for wild type (H) and somaclone (HS) grafted on 'Colt' (C) and 'Gisela 6'(G6) rootstock.

Genotype	Rootstock	Inflorescence flowers
H	'Colt'	2.8 a
	'G6'	6.3 b
HS	'Colt'	3.5 a
	'G6'	8.6 c

Note: Different letters represent significant differences for P > 0.05.

'Hedelfingen' (a) HS Somaclonal (b)

Fig. 1 Self-rooted trees (H and HS), transplanted on May 10th, 2005, after four years on May 8th, 2009.

Fig. 2 WT and HS trees grafted on 'G6' blooming at second growing season.

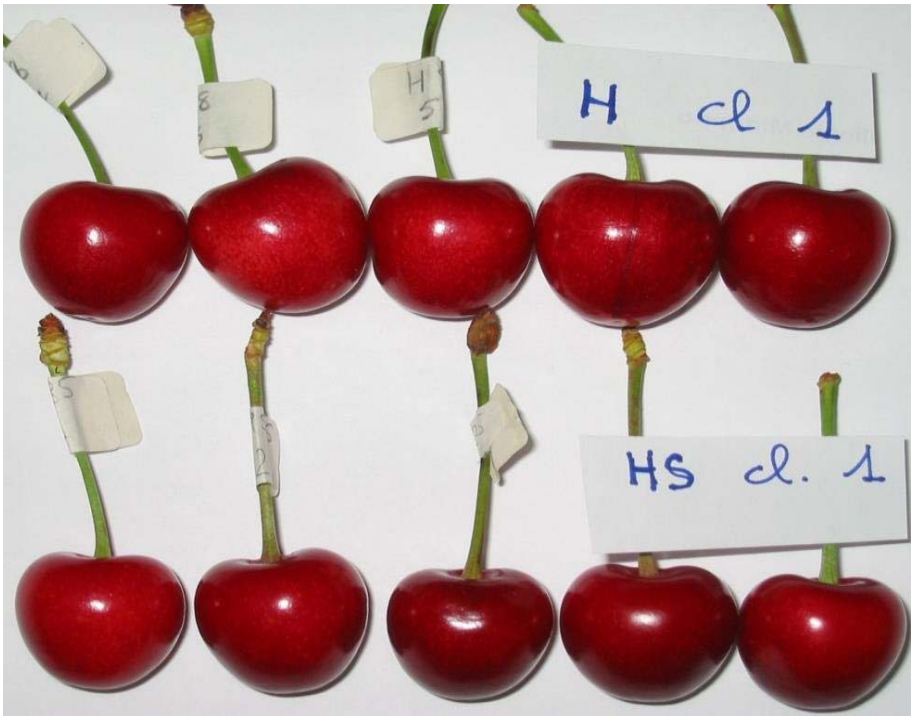

Fig. 3 First ripeness stage of cherry fruit collected on May 25th, 2013 (H = WT; HS = Somaclonal).

Fig. 4 Second ripeness stage of cherry fruit were collected on May 30th, 2013 (H = WT; HS = Somaclonal).

4. Conclusion

The somaclone HS was less vigorous than the wild type genotype, without any influence on natural tree's architecture based on crotch and extension angles, which did not differ between H and HS. HS was less productive but fruit quality did not differ from wild type.

The rootstock 'Gisela 6' have changed growth habit because, irrespective of genotype, that when grafting them has assumed an expanded habitus.

With regard to the vigor, rootstock has had more influence on the 'wild type' than Somaclonal, since 'Colt' induced an increase of trunk diameter and height, and a reduction of the length of the internodes. Two genotypes (WT and HS) were differently influenced by the rootstock in terms of size and shape of the leaves. 'Gisela 6' contributed to a significant increase in leaf surface.

Size and color of drupe are one of the most important quality factors for attaining a high price and in this view, any change due to somaclonal variation has to be carefully considered. Both fruit size, shape, the trend of fruit color change during the ripening process and the main parameters of fruit quality as assessed in the wild type and the Somaclone were the same. Although H and HS fruit final weight were the same, H reached its maximum quicker than HS.

'Gisela 6', from these preliminary data, had proved the most suitable rootstock for both genotypes since it induced early bearing and the production of a greater number of fruiting spurs.

References

[1] Jadczuk, E., and Sadowski, A. 1997. "Growth and Productivity of Self-rooted 'Schattenmorelle' Cherry Trees, Compared with Trees on Seedling Rootstocks." In *III International Cherry Symposium* 468: 377-84.

[2] Jain, S. M. 2001. "Tissue Culture-derived Variation in Crop Improvement." *Euphytica* 118 (2): 153-66.

[3] Goncalves, B., Moutinho-Pereira, J., Santos, A., Silva, A. P., Bacelar, E., Correia, C., et al. 2006. "Scion-rootstock Interaction Affects the Physiology and Fruit Quality of Sweet Cherry." *Tree Physiol.* 26 (1): 93-104.

[4] Gainza, F., Opazo, I., Guajardo, V., Meza, P., Ortiz, M., Pinochet, J., et al. 2015. "Rootstock Breeding in Prunus Species: Ongoing Efforts and New Challenges." *Chilean Journal of Agricultural Research* 75: 6-16.

[5] Krishna, H., Alizadeh, M., Singh, D., Singh, U., Chauhan, N., Sadh, R. K., et al. 2016. "Somaclonal Variations and Their Applications in Horticultural Crops Improvement." *3 Biotech* 6 (1): 1-18.

[6] Piagnani, M. C., Iacona, C., Intrieri, M. C., and Muleo, R. 2002. "A New Somaclone of Prunus Avium Shows

Diverse Growth Pattern under Different Spectral Quality of Radiation." *Biologia Plantarum* 45 (1): 11-7.

[7] Piagnani, M. C., Iacona, C., Intrieri, M. C., and Muleo, R. 2001. "A Somaclonal Variant in 'Hedelfinger' Sweet Cherry." *IV International Cherry Symposium* 667: 93-100.

[8] Piagnani, M. C., Chiozzotto, R., and Attanasio, G. 2011. "Effect of Rootstock on Vegetative and Riproduttive Growth of Somaclone 'HS' and Its Wild Type (CV 'Preliminary' Hedelfingen)." National Cherry Vignola Conference (MO), 29-30.

[9] Prinsi, B., Negri, A. S., Espen, L., and Piagnani, M. C. 2016. "Proteomic Comparison of Fruit Ripening between 'Hedelfinger' Sweet Cherry (Prunus Avium L.) and Its Somaclonal Variant 'HS'." *Journal of Agricultural and Food Chemistry* 64 (20): 4171-81.

Journal of Environmental Science and Engineering A 6 (2017) 370-376
doi:10.17265/2162-5298/2017.07.005

The Generation of Typical Meteorological Year and Climatic Database of Turkey for the Energy Analysis of Buildings

Serpil Yilmaz[1] and Ismail Ekmekci[2]

1. Department of Mechanical Engineering, The University of İstanbul Gedik, İstanbul 34876, Turkey

2. Department of Industrial Engineering, The University of İstanbul Commerce, İstanbul 34840, Turkey

Abstract: For sustainable development, a reduction in energy demand is essential. This could be achieved through improving energy efficiency, effective energy conservation and management. The weather conditions of a given region are the most important consideration for the proper design of space AC (Air Conditioning) systems. In this study, the typical meteorological year and climatic database of Turkey for the energy analysis of buildings were generated by SQL (Structured Query Language) database programmimg language. The Finkelstein-Schafer statistical method was applied to analyze the hourly measured weather data of a 23-year period (1989-2012) and select representative TMMs (Typical Meteorological Months). The selection criteria were based on 13 meteorological parameters. These parameters are the daily mean, maximum and minimum values and ranges of temperature, dew-point and wind velocity and the daily values of global solar radiation. According to results of TMY (Typical Meteorological Year), climatic database of Turkey including daily or hourly climate variables was created in SQL data tables.

Key words: HVAC (Heating, Cooling, Ventilating and Air Conditioning), typical meteorological year, heating degree hour, cooling degree hour.

1. Introduction

The design of energy requirements and thermal comfort of buildings requires an updated and very accurate climatological and solar database. A climatological and solar database is very important for calculation of energy efficiency. The hourly amounts of about 10-13 meteorological parameters such as solar radiation, dry bulb temperature, relative humidity, wind speed, atmospheric pressure, etc. are usually needed for energy simulation. A representative database for a year duration is known as a TMY (Typical Meteorological Year), a term mainly used in the USA, or a TRY (Test Reference Year) or a DRY (Design Reference Year), terms mainly used in Europe. TMY, TRY or DRY consists of individual months of meteorological data sets selected from different years over the available data period, which is called a long-term measured data.

The primary objective of these methods is to select single years or single months from a multi-year database, preserving a statistical correspondence. This means that the occurrence and the persistence of the weather should be as similar as possible in the TMY to all available years. These different TMY methodologies have been developed with selection criteria based on solar radiation or on solar radiation together with other meteorological variables [1-5].

The literature review conducted in this work shows that one of the most common methodologies for generating a TMY is the one proposed by Hall, I. J., et al. [4] using the FS (Filkenstein-Schafer) statistical method. The other methodologies for generating TMY use a modified version of it. This method is an empirical approach that selects individual months from different recorded years. The selection criteria

Corresponding author: Serpil Yilmaz, Ph.D., assistant professor, research field: HVAC (Heating, Cooling, Ventilating and Air Conditioning).

were based on 13 meteorological parameters. These parameters were the daily mean, maximum and minimum values and ranges of temperature, dew-point and wind velocity and the daily values of global solar radiation. However, four of 13 parameters were considered to be less effective, and therefore, are given zero weight. These variables are the ranges of daily dry-bulb temperature, wet-bulb temperature and wind speed, and daily minimum wind speed. Except for a few changes to the weighting criteria, which account for the relative importance of the solar radiation and meteorological elements, there has been no change in the original methodology which has been adopted by different countries [6-9].

2. Review on Typical Meteorological Year

A TMY consists of the months selected from the individual years and sorted to form a complete year. In the literature, there are many attempts to produce weather databases for different locations. The main objective of these methods is to select representative months from the multi-year database. This methodology has been adopted by different countries: for example, by date of publication, for Holmet Stations [10], Athens [11], Egypt [12], Ibadan, Nigeria [13], Hong Kong [14], Nicosia, Cyprus [15], Saudi Arabia [16], Malaysia [17] and Damascus, Syria [18].

Recently, ASHRAE (The American Society of Heating, Refrigerating and Air-Conditioning Engineers) has started an international project to develop TMY data throughout the world, the IWEC (International Weather Year for Energy Calculations) [5]. Most recently, using the FS method, Kalogirou, S. A. [19] developed TMYs for the city of Nicosia, Cyprus. The study of Kalogirou, S. A. [19] included additional variables such as illuminance, visibility, precipitation and snow fall data. The objective of the present work is to select and implement TMY generating methodologies using long term hourly measured meteorological and global solar radiation data.

For Turkey, only three attempts have been found in the literature for the generation of TMY datasets [20-22]. Pusat, S., et al. [21] generated TMY for 8 cities. Ecevit, A., et al. [20] generated the TMY for Ankara. They stated that solar radiation data were unreliable in Turkey [20, 21]. Therefore, they evaluated the possibility of using the daily sunshine duration or the ratio of the daily sunshine duration to the day-length instead of daily global solar radiation, as the ninth parameter, in obtaining TMY [20, 21]. They used the data of Ankara covering the period 1979-1999 [20]. In the paper of Uner, M. and Ileri, A. [22], TMYs for 23 cities representing demographic and climatic conditions of Turkey were investigated by using actual recordings (1990-1996). They generated the typical meteorological database of 23 locations for building simulations and air-conditioning design [22]. The only deficiency in this study is the number of years used in the generation of TMY. There isn't enough study to generate TMY datasets for Turkish locations in the literature. TMY datasets was generated just for Ankara, and number of years used is not enough for TMY generation.

3. Problem Definition in Measurements and Data

In this study, the meteorological data was obtained from DMI (The State Meteorological Affairs General Directorate) and covered a period of 1989-2012 for 81 cities throughout the Turkey. Meteorological stations are located in city centers and there is generally only one station in each city. There were missing and invalid measurements in the data and they were filled as null. So, the data were checked for wrong entries and missing data. The missing and invalid measurements, accounting for approximately 0.30% of the whole database, were replaced with the values of preceding or subsequent days by interpolation. In the calculations, the year was excluded from the database if more than 15 days measurements were not available in a month.

4. TMY Selection Method

For each station, nine daily meteorological parameters: maximum air temperature (T_{max}), minimum air temperature (T_{min}), mean air temperature (T_{mean}), maximum air relative humidity (RH_{max}), minimum air relative humidity (RH_{min}), mean air relative humidity (RH_{mean}), maximum wind speed (W_{max}), mean wind speed (W_{mean}) and global solar radiation (G) were employed to create an indicator for selecting TMMs (Typical Meteorological Months). The weighting factors used are selected according to existing experience on the influence of the meteorological parameters used on the simulated application. Three sets of weighting factors, all oriented towards energy simulation applications were used, as shown in Table 1.

In the first step, for a given parameter xi, a long-term CDF_m (Cumulative Distribution Function) of xi for each month covering the period of 23-year (1989-2012) was created.

A short-term $CDF_{y,m}$ of xi for year y and month m was also generated. FS statistics are the most common methodology for creating CDF functions while generating typical weather data. This method is an empirical methodology for selecting individual months from different years over the available period. According to FS statistics [23], if a number, n, of observations of a variable X is available and has been sorted into an increasing order X_1, X_2,…, Xn, the CDF of this variable is given by a function Sn(X) which is defined as:

$$S_n(\chi) = \begin{cases} 0 & \text{for } X < X_1 \\ (k - 0.5)/n & \text{for } X_\lambda < \chi < X_{\lambda+1} \\ 1 & \text{for } X > X_n \end{cases} \quad (1)$$

The FS by which comparison between the long-term CDF of each month and the CDF for each individual year of the month was done is given by Eq. (2):

$$FS_{Xi}(y,m) = \frac{1}{N_d}\sum_{j=1}^{N_d}\left| CDF_m(X_{ij}) - CDF_{y,m}(X_{i,j}) \right| \quad (2)$$

where $FS_{Xi}(y,m)$ is the FS statistics of the parameter X_i for year y and month m; j is interval number of data and N_d is the total number of data intervals.

In the second step, the weighted sums of FS_{Xi} were computed by:

$$WS(y,m) = \frac{1}{N_P}\sum_{i=1}^{N_p} WF_{X_i} . FS_{x_i}(y,m) \quad (3)$$

$$\sum_{i=1}^{N_p} WF_{x_i} = 1 \quad (4)$$

where WF_{x_i} is the weighting factors for the FS of the variable X_i and N_p is the total number of the parameters. In this case, the weighting factor for T_{max}, T_{min}, Rh_{max} and RH_{min} is 0.04; for T_{mean}, RH_{mean}, W_{max} and W_{mean} is 0.08 and for global radiation is 0.5. All individual months are ranked in ascending order of WS (Weighted Sums) values [23].

Table 1 Weighting factors for TMY type.

Present (FS)				Weather index
[23]	[24]	[17]	[25, 26]	
1/24	5/100	5/100	1/20	Maximum dry bulb temperature
1/24	5/100	5/100	1/20	Minimum dry bulb temperature
2/24	30/100	30/100	2/20	Mean dry bulb temperature
1/24		2.5/100	1/20	Maximum dew point temperature
1/24		2.5/100	1/20	Minimum dew point temperature
2/24		5/100	1/20	Mean dew point temperature
2/24	5/100	5/100	1/20	Maximum wind speed
2/24	5/100	5/100	1/20	Mean wind speed
12/24	40/100	40/100	5/20	Total horizontal solar radiation
			5/20	Direct solar radiation
	10/100			Relative humidity

Table 2 TMY values for each city of Turkey.

City code	City name	Typical meteorological years											
		Months (1-12)											
		1	2	3	4	5	6	7	8	9	10	11	12
17020	Bartin	2004	2005	2004	2005	2004	2008	2003	1989	2003	2005	2004	2005
17022	Zonguldak	2004	2008	2012	1990	1997	2004	2005	1989	2012	1989	2012	1994
17026	Sinop	2004	1990	2011	1990	2005	2002	1990	1990	2008	1989	2007	1989
17030	Samsun	1995	1998	1994	2001	1995	1998	1995	1999	1989	1997	1995	1997
17033	Ordu	2012	1990	2004	1995	2009	1992	2009	1991	2007	1997	2006	1993
17034	Giresun	2009	1989	2009	1990	2012	1990	2012	1989	2009	1990	2009	1990
17037	Trabzon	2004	1989	2004	1990	2004	1989	2003	1993	2004	1989	2004	1989
17040	Rize	2009	1990	2010	1990	2010	1991	2009	1995	2009	1990	2009	1990
17045	Artvin	2011	1990	2007	1990	2010	1991	2008	1995	1995	1989	2012	1991
17046	Ardahan	1998	2002	1994	1990	2011	2009	2011	1992	2009	1989	2009	2003
17050	Edirne	2011	1994	2011	1992	2011	2002	2010	2010	2010	1994	2009	1993
17052	Kirklareli	2008	1989	2011	1990	2011	1990	2011	1989	2011	1989	2011	1989
17056	Tekirdag	2011	1990	2011	1990	2011	1993	2010	1998	2009	1989	2008	1989
17062	Istanbul	2006	1990	2006	1990	2005	1990	1991	1994	2007	1991	2001	1990
17066	Kocaeli	2009	1990	2011	1990	2009	1990	2010	2007	2007	1990	2012	1990
17069	Sakarya	2011	1990	2012	1990	2008	1992	1998	2012	2006	1990	2012	1990
17070	Bolu	2009	1990	2009	1992	2011	1993	2000	1994	1998	1990	2012	1990
17072	Duzce	2009	1989	2011	1990	2008	1993	2009	1993	2006	1990	2009	1990
17074	Kastamonu	2012	1990	2011	1992	2012	2000	2003	2003	2010	1990	2009	1989
17078	Karabuk	2010	2008	2011	2000	2011	2009	2010	2010	2000	2000	2008	2007
17080	Cankiri	2009	1990	2005	1990	1990	1990	2002	1991	1991	1990	2009	1990
17084	Corum	2009	1990	2006	1990	2010	1990	1999	1989	2003	1989	2008	1989
17085	Amasya	2004	1994	2010	1990	2005	1990	2008	1994	2010	1989	2008	1989
17086	Tokat	2011	1989	2011	2006	2009	1989	2010	1989	2009	1990	2009	1990
17088	Gumushane	2007	2004	1991	1990	2010	1990	2001	1989	2008	1989	2009	1990
17089	Bayburt	2012	1990	2011	1990	2011	1990	2011	1991	2006	1990	2008	1990
17090	Sivas	2011	1989	2007	1992	2010	1993	2008	2008	2006	1990	2011	1995
17094	Erzincan	2011	2003	2010	1995	2010	1989	1998	1989	2009	1992	2009	1997
17096	Erzurum	2006	1995	2007	1990	2005	1990	2006	2005	2006	1990	2007	1997
17097	Kars	2000	1992	2007	1993	2009	1994	2008	1991	2000	1992	2003	1991
17099	Agri	2009	1989	2009	2000	2010	2009	1996	1994	2009	1990	2009	2003
17100	Igdir	2009	1990	2009	1990	2009	1990	2009	2003	2005	1989	2009	1990
17112	Canakkale	2011	1991	2011	1992	2011	2010	1994	2008	2010	1990	2012	1989
17116	Bursa	2011	1991	2011	1990	2005	1990	1999	1989	2009	1990	2009	1990
17119	Yalova	2011	1990	2011	1990	2011	1990	2011	1994	2011	1990	2009	1994
17120	Bilecik	2011	1990	2011	1990	2011	1990	2011	1994	2011	1990	2009	1994
17126	Eskisehir	2012	2012	2011	2010	2009	2007	2011	2007	2011	2007	2008	2012
17130	Ankara	2007	1990	2007	1992	2006	2011	2004	2000	2004	1990	2008	1990
17135	Kirikkale	2009	1989	2007	1990	2010	1989	2008	1989	2006	1990	2012	1990
17140	Yozgat	2012	1990	2010	1991	2009	1990	2011	1989	2008	1990	2012	1989
17152	Balikesir	1993	1990	1995	1990	1990	1991	1994	1996	1995	1990	1995	1989

(Table 2 continued)

City code	City name	Typical meteorological years											
		Months (1-12)											
		1	2	3	4	5	6	7	8	9	10	11	12
17155	Kutahya	2008	1990	2007	1998	2009	1995	1999	1995	2006	1989	2012	1990
17160	Kirsehir	2009	1990	1991	1990	2005	1989	1999	1992	1998	1990	2009	1989
17165	Tunceli	2009	1991	2009	1991	2007	1990	2001	1998	2008	2007	2009	1991
17172	Van	2006	1991	2007	1993	2007	1994	1996	1999	2006	1990	2008	1990
17186	Manisa	2011	1991	2012	1990	2006	1991	2005	1993	1995	1991	2005	1989
17188	Usak	2011	2006	1999	2004	2012	1996	2006	1999	2011	1990	2012	1989
17190	Afyonkarahisar	2004	1990	2011	2005	2009	1993	2010	1989	2000	1990	2011	1989
17192	Aksaray	2011	1993	2008	1990	2010	2007	2007	2007	2009	1990	2009	1989
17193	Nevsehir	1996	1989	2011	1990	2011	1989	2011	1989	1998	1989	2009	1989
17196	Kayseri	2009	1989	2009	1992	2009	1989	2006	1996	2009	1990	2009	1990
17199	Malatya	2012	1994	2011	1993	2012	1995	2006	1995	2009	1992	2008	1993
17201	Elazig	2009	1991	2011	1990	2009	1991	2004	1998	1994	1990	2009	1993
17203	Bingol	2011	1991	2009	1990	2010	1995	2004	2002	2008	1990	2009	1991
17204	Mus	2006	1993	2009	1990	2010	1991	2006	2004	2008	1991	2008	1991
17207	Bitlis	2009	1993	2009	2004	2008	1997	2006	2000	2008	1991	2009	1997
17210	Siirt	2009	1991	2011	1996	2010	1995	2009	2005	2005	1990	2007	2000
17220	Izmir	2011	1990	2012	1990	2009	2012	1996	2011	1990	1990	2010	1989
17234	Aydin	2007	1991	2011	1990	2009	2009	2000	1992	2011	1991	2012	1997
17237	Denizli	2011	1990	2011	1990	2010	1997	1998	1994	2011	1998	2007	1995
17238	Burdur	2011	1990	2011	1990	2009	1993	2006	2006	2006	1990	2012	1990
17240	Isparta	2006	1990	2005	1999	2012	2010	2002	2007	1993	2007	2012	1990
17244	Konya	2004	1990	1994	1991	1991	1995	1991	2002	2002	1997	2001	1997
17246	Karaman	2009	1990	2011	1990	2009	1991	2007	1996	2006	1990	2009	2003
17250	Nigde	1996	1989	2005	1990	2010	1991	1999	1996	2009	1989	2009	1997
17255	Kahramanmaras	2011	1991	2007	1991	2008	2007	1998	2008	2006	1991	2012	1997
17261	Gaziantep	2006	1991	2011	1991	2009	1995	2004	1999	2006	1994	2008	1993
17262	Kilis	2006	1990	1991	1991	2005	2005	1998	1992	2006	1991	2012	1993
17265	Adiyaman	2009	1990	2011	1991	2004	2002	1990	1990	2001	1998	2009	1998
17270	Sanliurfa	2005	1990	2010	1991	2010	1995	2009	1991	2007	1990	2005	2005
17275	Mardin	2006	1990	2011	1991	2011	1994	2011	1989	2011	1990	2009	1989
17280	Diyarbakir	2009	1990	2011	1991	2010	2001	2006	2001	2008	1990	2009	1999
17282	Batman	2009	1990	2011	1990	2011	2010	2007	2007	2011	1990	2009	1990
17285	Hakkari	2011	1990	2012	1993	2010	1989	2011	1989	2010	1989	2009	1990
17287	Sirnak	2011	2000	2011	2003	2011	2002	2007	2001	2011	1991	2009	1999
17292	Mugla	2011	1990	2011	2001	2012	2002	1996	2000	2010	1991	2009	1989
17300	Antalya	1995	2006	1998	2005	1998	2006	1999	2002	1998	2006	1997	2004
17340	Mersin	2009	2004	2009	1991	2009	1993	2007	1999	2009	1990	2009	1990
17351	Adana	2006	1990	2011	1990	2010	1993	2010	1996	2009	1989	2007	1989
17355	Osmaniye	2012	1990	2012	1990	2012	1989	2012	1992	1997	1990	1997	1990
17372	Hatay	2006	1991	2007	2005	2009	2003	2007	2007	2007	1991	2007	1989

5. Results

The calculated TMY values for each city of Turkey are on Table 2.

6. Conclusions

Energy consumption in Turkey is increasing continuously parallel to its development. Because of its limited energy resources, Turkey is heavily dependent on imported oil and gas. Therefore, every means to use energy in a much more rational way should be taken into consideration. HVAC (Heating, Cooling, Ventilating and Air Conditioning) systems are major energy users in residential and commercial buildings.

The first step in the design of air-conditioning systems is the calculation of heating and cooling loads of the building that depend on its characteristics, the indoor conditions to be maintained and the outside weather conditions. If the air-conditioning system is expected to provide the indoor conditions specified (comfort conditions) at all times, it should be designed for peak conditions that are determined by the most extreme weather data recorded for the locality in which the building is located. This approach, however, will result in oversized air conditioning equipment, which in turn, will increase the initial equipment cost and the operating cost. It is very important to represent the climate of a location. In this study, TMY for 81 cities of Turkey was calculated. It will be very useful source for building simulations to estimate the annual energy consumptions of buildings.

References

[1] Klein, S. A., Cooper, P. I., Freeman, T. L., Beekman, D. M., Beckman, W. A., and Duffie, J. A. 1975. “A Method of Simulation of Solar Processes and Its Applications.” *Solar Energy* 17 (1): 29-37.

[2] Klein, S. A., Beckman, W. A., and Duffie, J. A. 1976. “A Design Procedure for Solar Heating Systems.” *Solar Energy* 18 (2): 113-27.

[3] Schweitzer, S. 1978. “A Possible “Average” Weather Year on Israel’s Coastal Plain for Solar System Simulations.” *Solar Energy* 21 (6): 511-5.

[4] Hall, I. J., Prairie, R. R., Anderson, H. E., and Boes, E. C. 1978. *Generation of a Typical Meteorological Year* (No. SAND-78-1096C; CONF-780639-1). Sandia Laboratories, Albuquerque, NM.

[5] Crow, L. W. 1984. “Weather Year for Energy Calculations.” *ASHRAE J. (United States)*: 26.

[6] Feuermann, D., Gordon, J. M., and Zarmi, Y. 1985. “A Typical Meteorological Day (TMD) Approach for Predicting the Long-Term Performance of Solar Energy Systems.” *Solar Energy* 35 (1): 63-9.

[7] Wilcox, S., and Marion, W. 2008. *Users Manual for TMY3 Data Sets*. National Renewable Energy Laboratory Technical report, NREL/TP-581-43156.

[8] Gazela, M., and Mathioulakis, E. 2001. “A New Method for Typical Weather Data Selection to Evaluate Long-Term Performance of Solar Energy Systems.” *Solar Energy* 70 (4): 339-48.

[9] Yang, H. X., and Lu, L. 2004. “The Development and Comparision of Typical Meteorological Years for Building Energy Simulation and Renewable Energy Applications.” *ASHRAE Trans.* 110 (2): 424-31.

[10] Bahadori, M. N., and Chamberlain, M. J. 1986. “A Simplification of Weather Data to Evaluate Daily and Monthly Energy Needs of Residential Buildings.” *Solar Energy* 36 (6): 499-507.

[11] Pissimanis, D., Karras, G., Notaridou, V., and Gavra, K. 1988. “The Generation of a “Typical Meteorological Year” for the Vity of Athens.” *Solar Energy* 40 (5): 405-11.

[12] Shaltout, M. A. M., and Tadros, M. T. Y. 1994. “Typical Solar Radiation Year for Egypt.” *Renewable Energy* 4 (4): 387-93.

[13] Fagbenle, R. L. 1995. “Generation of a Test Reference Year for Ibadan, Nigeria.” *Energy Conversion and Management* 36 (1): 61-3.

[14] Wong, W. L., and Ngan, K. H. 1993. “Selection of an “Example Weather Year” for Hong Kong.” *Energy and Buildings* 19 (4): 313-6.

[15] Petrakis, M., Kambezidis, H. D., Lykoudis, S., Adamopoulos, A. D., Kassomenos, P., Michaelides, I. M., et al. 1998. “Generation of a “Typical Meteorological Year” for Nicosia, Cyprus.” *Renewable Energy* 13 (3): 381-8.

[16] Said, S. A. M., and Kadry, H. M. 1994. “Generation of Representative Weather—Year Data for Saudi Arabia.” *Applied Energy* 48 (2): 131-6.

[17] Rahman, I. A., and Dewsbury, J. 2007. “Selection of Typical Weather Data (Test Reference Years) for Subang, Malaysia.” *Building and Environment* 42 (10): 3636-41.

[18] Skeiker, K. 20014. “Generation of a Typical Meteorological Year for Damascus Zone Using the Filkenstein-Schafer Statistical Method.” *Energy*

Conversion and Management 45 (1): 99-112.

[19] Kalogirou, S. A. 2003. "Generation of Typical Meteorological Year (TMY-2) for Nicosia, Cyprus." *Renewable Energy* 28 (15): 2317-34.

[20] Ecevit, A., Akinoglu, B. G., and Aksoy, B. 2002. "Generation of a Typical Meteorological Year Using Sunshine Duration Data." *Energy* 27 (10): 947-54.

[21] Pusat, S., Ekmekci, I., and Akkoyunlu, M. T. 2015. "Generation of Typical Meteorological Year for Different Climates of Turkey." *Renewable Energy* 75: 144-51.

[22] Uner, M., and Ileri, A. 2000. "Typical Weather Data of Main Turkish Cities for Energy Applications." *Int. J. Energy Res.* 24 (8): 727-48.

[23] Finkelstein, J. M., and Schafer, R. E. 1971. "Improved Goodness-of-Fit Tests." *Biometrika* 58 (3): 641-5.

[24] ASHRAE Handbook. 1997. "HVAC Applications." *ASHRAE Handbook Fundamentals*. Atlanta: ASHRAE.

[25] Bahadori, M. N., and Chamberlain, M. J. 1986. "A Simplification of Weather Data Daily and Monthly Energy Needs of Residential Buildings." *Solar Energy* 36 (6): 499-507.

[26] Siurna, D. L., D'Andrea, L. J., and Hollands, K. G. T. 1984. "A Canadian Representative Meteorological Year for Solar System Simulation." In *Proceedings of 10th Annual Conference of the Solar Energy Society of Canada (SESCI'84), Calgory*, 2-6.

Journal of Environmental Science and Engineering A 6 (2017) 377-380
doi:10.17265/2162-5298/2017.07.006

Optimum Determination of Partial Transmission Ratios of Mechanical Driven Systems Using a V-belt and a Helical Gearbox with Second-Step Double Gear-Sets

Nguyen Khac Tuan[1] and Vu Ngoc Pi[2]

1. Automotive and Power Machinery Faculty, Thai Nguyen University of Technology, Thai Nguyen 23000, Vietnam

2. Mechanical Engineering Faculty, Thai Nguyen University of Technology, Thai Nguyen 23000, Vietnam

Abstract: This paper presents a study on the optimum determination of partial transmission ratios of a mechanical drive system using a V-belt and a helical gearbox with second-step double gear-sets in order to get the minimum size of the system. The chosen objective function was the cross section dimension of the system. In the optimization problem, the design equation for pitting resistance of a gear set was investigated and equations on moment equilibrium condition of a mechanic system including a V-belt and a helical gearbox with second-step double gear-sets and their regular resistance condition were analysed. Based on the results of the study, effective formulas for calculation of the partial ratios of the V-belt and a helical gearbox with second-step double gear-sets were proposed. By using explicit models, the partial ratios can be determined accurately and simply.

Key words: Transmission ratio, gearbox design, optimum design, V-belt drive, helical gearbox.

1. Introduction

In the problem of optimum gearbox design, optimum calculation of partial transmission ratios of the gearbox is one of the most important works. This is because the partial ratios are main factors affecting the dimension, the weight as well as the cost of the gearbox [1]. Consequently, optimum determination of the partial ratios of a gearbox has been subjected to many researches.

Till now, a lot of studies on the determination of the partial ratios of gearboxes have been done. The partial ratios were predicted for different gearbox types, such as for helical gearboxes [1-5], for bevel-helical gearboxes [1, 4, 6, 7] and for worm-gearboxes [4, 8]. In addition, many methods have been used for determining optimum partial ratios. These methods are the graph method [1, 2], the “practical method” [3] and modeling method [4-8].

Corresponding author: Vu Ngoc Pi, associate professor, Ph.D., main research fields: optimum design of machine elements and abrasive machining.

From above analysis, it is found that there have been many studies on the determination of the partial ratios for different types of gearboxes. However, until now, there was only a study for mechanical driven systems using a V-belt and a two-step helical gearbox [9]. There have not been studies for mechanical driven systems using a V-belt and a helical gearbox with second-step double gear-sets. This paper presents a study on optimum determination of partial ratios for mechanical systems using a V-belt and a helical gearbox with second-step double gear-set for getting the minimum system cross-sectional dimension.

2. Calculation of Optimum Partial Transmission Ratios

For a helical gearbox with second-step double gear-sets (Fig. 1), the cross-sectional dimension is minimum when d_{w21} and d_{w22} satisfy Eq. (1) [1].

$$d_{w21} = d_{w22} \quad (1)$$

From Eq. (1) and Fig. 1, for a mechanical drive system using a V-belt and a helical gearbox with

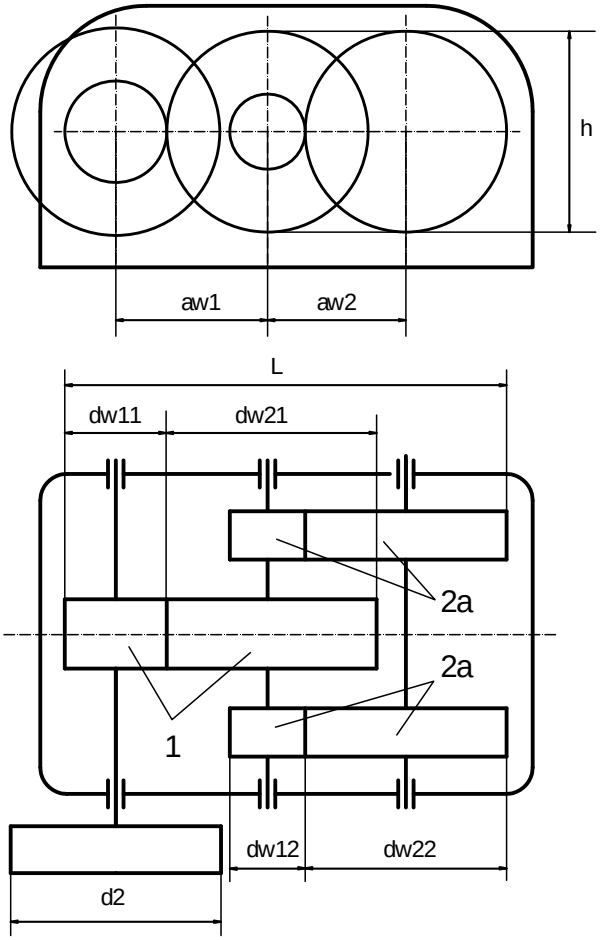

Fig. 1 Calculation chema for optimum determination of partial transmission ratios.

second-step double gear-sets, the cross-sectional dimension of the system is minimum when:

$$d_2 = d_{w21} = d_{w22} \tag{2}$$

Where d_2 is driven pulley diameter (mm); d_{w21} and d_{w22} are driven diameters of two gear units (mm).

For a helical gearbox with second-step double gear-sets, the optimum partial gear ratios u_1 and u_2 have been determined by Eq. (3) [5]:

$$u_2 = 1.2776 \cdot \sqrt[3]{\frac{K_{c2} \cdot \psi_{ba2}}{\psi_{ba1}} \cdot u_g} \tag{3}$$

In which u_g is the transmission ratio of the gearbox; ψ_{ba1} and ψ_{ba2} are coefficients of helical gear face width of steps 1 and 2; K_{c2} is coefficient; K_{c2} is 1.1 to 1.3 [5]. For this helical gearbox, it can be chosen as ψ_{ba1} = 0.3 and ψ_{ba2} = 0.35 [10]. Choosing K_{c2} = 1.2 and substituting ψ_{ba1}, ψ_{ba2} and K_{c2} into Eq. (3) gives Eq. (4):

$$u_2 = 1.3884 \cdot u_g^{1/3} \tag{4}$$

Eq. (4) is used to determine the partial ratio u_2 of the second step. The partial ratio u_1 of the first step can be calculated by Eq. (5):

$$u_1 = u_g / u_2 \tag{5}$$

From above analysis, it is found that for finding the optimum partial ratios of the systems in order to get the minimum system cross section, it is necessary to determine the diameters d_2 and d_{w22}.

2.1 Determining the Driven Pulley Diameter d_2

For a V-belt set, from tabulated data for determining allowable power [10], the regression model for calculation of driver diameter d_1 (with the determination coefficient R^2 = 0.9156) was found:

$$d_1 = 269.7721 \cdot [P_1]^{0.7042} / v^{0.5067} \tag{6}$$

Theoretically, the peripheral velocity of the belt can be determined as Eq. (7):

$$v = \pi \cdot d_1 \cdot n_1 / 60000 \tag{7}$$

From Eqs. (6) and (7), the diameter of the driver pulley can be determined by Eq. (8):

$$d_1 = 1093.8 \cdot [P_1]^{0.7923} / n_1^{0.6369} \tag{8}$$

Also, the diameter of driven pulley of a V-belt drive is calculated by Eq. (9) [10]:

$$d_2 = u_b \cdot d_1 \cdot (1 - \varepsilon) \tag{9}$$

Substituting Eq. (8) into Eq. (9) gives Eq. (10):

$$d_2 = 1093.8 \cdot u_b \cdot (1 - \varepsilon) \cdot [p_1]^{0.7923} / n_1^{0.6369} \tag{10}$$

Where ε is slippage coefficient; $\varepsilon = 0.01 \ldots 0.02$ [10]; u_b is the transmission ratio of the V-belt set; $[P_1]$ is the allowable power of the drive (kW); $[P_1]$ is calculated by Eq. (11):

$$[P_1] = n_1 \cdot [T_1] / (9.55 \cdot 10^6) \tag{11}$$

Choosing $\varepsilon = 0.015$ and substituting it and Eq. (11) into Eq. (10) gives Eq. (12):

$$d_2 = 0.0032 \cdot u_b \cdot n_1^{0.1554} \cdot [T_1]^{0.7923} \quad (12)$$

2.2. Determining the Driven Diameter d_{w22}

For the second-step with double gear-sets, the driven diameter can be determined by Eq. (13) [5]:

$$d_{w22} = \left[\frac{2.0786 \cdot [T_{out}] \cdot u_2}{\psi_{ba2} \cdot [K_{02}]} \right]^{1/3} \quad (13)$$

Where ψ_{ba2} = 0.35 (see section 2);

$$K_{02} = [\sigma_{H2}]^2 / \left(K_{H2} (Z_{M2} Z_{H2} Z_{\varepsilon 2})^2 \right) \quad (14)$$

In which, $[\sigma_{H2}]$—Allowable contact stress of the second-step gear set (MPa); For a helical gear set, $[\sigma_{H2}]$ can be calculated by Eq. (15) [10]:

$$[\sigma_{H2}] = \left([\sigma_H]_1 + [\sigma_H]_2 \right) / 2 \quad (15)$$

Where $[\sigma_H]_1$ and $[\sigma_H]_2$ are the allowable contact stress of pinion and gear of the second step gear set (MPa). $[\sigma_H]_1$ is determined by Eq. (16):

$$[\sigma_H]_1 = \sigma^0_{H\lim 1} \cdot K_{HL} / S_H \quad (16)$$

In Eq. (16), $\sigma^0_{H\lim 1}$ is allowable contact stress for based stress cycle life of the pinion: $\sigma^0_{H\lim 1} = 2 \cdot HB_1 + 70$; HB_1 is Brinell hardness of the pinion; K_{HL} is the stress cycle life factor; S_H is the safety factor. Since the material of the pinion is medium carbon steel 1045, it was found $HB_1 = 250$, $K_{HL} = 1$ and $S_H = 1.1$ [10].

Substituting $\sigma^0_{H\lim 1}$, K_{HL} and S_H into Eq. (16) gives $[\sigma_H]_1 = 518.18$ (MPa).

Calculating the same way for the gear gives $[\sigma_H]_2 = 490.91$ (MPa).

Substituting values of $[\sigma_H]_1$ and $[\sigma_H]_2$ into Eq. (15) gives $[\sigma_{H2}] = 504.55$ (MPa).

K_{H2}—Contact load factor for pitting resistance; Since $K_{H2} = 1.1 - 1.3$ [10], authors can choose $K_{H2} = 1.2$;

Z_{M2}—Material factor; Since the pinion and gear are made from steel, Z_{M2} is 274 ($MPa^{1/3}$) [10];

Z_{H2}—Surface condition factor; With the pinion and gear are standard and the helix angles are $8^0 \div 20^0$, Z_{H2} = $1.74 \div 1.67$ [10]. Therefore, authors can choose $Z_{H2} = 1.71$;

$Z_{\varepsilon 2}$—Loading sharing factor: $Z_{\varepsilon 2} = \left(1/\varepsilon_\alpha\right)^{1/2}$ [10] with ε_α is contact ratio. ε_α can be calculated by Eq. (17) [10]:

$$\varepsilon_\alpha = \left[1.88 - 3.2 \left(1/z_1 + 1/z_2 \right) \right] \cdot \cos\beta \quad (17)$$

With the helix angles are $8^0 \div 20^0$ and the number of teeth of pinion and gear are 15 to 90, the value of the transverse contact ratio is $Z_{\varepsilon 2} = 0.7628 \div 0.8344$. Therefore, the value of $Z_{\varepsilon 2}$ can be chosen as the average of these values, that is, $Z_{\varepsilon 2} = 0.7986$.

Substituting values of $[\sigma_{H2}]$, K_{H2}, Z_{M2}, Z_{H2} and $Z_{\varepsilon 2}$ into Eq. (14) gives Eq. (18):

$$K_{02} = 504.55^2 / \left(1.2 \cdot (274 \cdot 1.71 \cdot 0.7986)^2 \right) = 1.5152 \quad (18)$$

Substituting $\psi_{ba2} = 0.35$ and $K_{02} = 1.5152$ into Eq. (13) gives Eq. (19):

$$d_{w22} = 1.5767 \cdot [T_{out}]^{1/3} \cdot u_2^{1/3} \quad (19)$$

2.3 Determining the Partial Ratios

Eqs. (2), (12) and (19) give Eq. (20):

$$0.0032 \cdot u_b \cdot n_1^{0.1554} \cdot [T_1]^{0.7923} = 1.5767 \cdot [T_{out}]^{1/3} \cdot u_2^{1/3} \quad (20)$$

Theoretically, the permissible torque on the drive shaft $[T_1]$ can be calculated from permissible torque on the output shaft $[T_r]$ by Eq. (21):

$$[T_1] = [T_r] / \left(u_t \cdot \eta_t \right) \quad (21)$$

Where u_t is the total transmission ratio of the system; η_t is the total efficiency of the system:

$$\eta_t = \eta_d \cdot \eta_{br}^2 \eta_o^3 \quad (22)$$

In which, η_d is V-belt efficiency (η_d is from 0.956 to 0.96 [2]); η_{br} is helical gear transmission efficiency (η_{br} is from 0.96 to 0.98 [2]); η_o is transmission efficiency of a pair of rolling bearing (η_o is from 0.99 to 0.995 [2]). Choosing $\eta_d = 0.955$, $\eta_{br} = 0.97$ and $\eta_o = 0.992$ [10] and substituting Eqs. (4), (21) and (22) into Eq. (20) with the note that

$u_g = u_t / u_b$ gives Eq. (23):

$$u_b = 266.3906 \cdot \left[T_{out}\right]^{-0.4962} \cdot n_1^{-0.1872} \cdot u_t^{0.9126} \quad (23)$$

Eq. (23) is used to calculate the speed ratio of the V-belt driver. After having u_b, the ratio of the gearbox is calculated by $u_g = u_t / u_b$ and the partial speed ratios of the gearbox u_1 and u_2 can be found by Eqs. (5) and (4), respectively.

3. Conclusions

The minimum system cross-sectional dimension of a mechanical drive system using a V-belt and a helical gearbox with second-step double gear-sets can be obtained by optimum splitting the total transmission ratio of the system.

Models for determining the partial ratios of the V-belt and the helical gearbox in order to get the minimum cross-sectional dimension of the system were proposed.

By using explicit models, the partial ratios of the V-belt driver and the helical gear units can be determined accurately and simply.

References

[1] Kudreavtev, V. N., Gierzaves, I. A., and Glukharev, E. G. 1971. "Design and Calculus of Gearboxes." Mashinostroenie Publishing, Sankt Petersburg.

[2] Petrovski, A. N., Sapiro, B. A., and Saphonova, N. K. 1987. "About Optimal Problem for Multi-Step Gearboxes." *Vestnik Mashinostroenie* 10: 13-4.

[3] Milou; G., Dobre, G., Visa, F., and Vintila, H. 1996. "Optimal Design of Two Step Gear Units, Regarding the Main Parameters." *VDI BERICHTE* 1230: 227-44.

[4] Pi, V. N., and Tuan, N. K. 2016. "Optimum Determination of Partial Transmission Ratios of Three-Step Helical Gearboxes for Getting Minimum Cross Section Dimension." *Journal of Environmental Science and Engineering A* 11 (4): 570-3.

[5] Pi, V. N. 2008. "A Study on Optimal Determination of Partial Transmission Ratios of Helical Gearboxes with Second-Step Double Gear-Sets." *Proc. of World Academy of Science* 27: 113-6.

[6] Pi, V. N. 2000. "A New and Effective Method for Optimal Calculation of Total Transmission Ratio of Two Step Bevel-Helical Gearboxes." In *International Colloquium on Mechannics of Solids, Fluids, Structures & Interaction Nha Trang, Vietnam*, 716-9.

[7] Pi, V. N., Binh, N. D., Dac, V. Q., and The, P. Q. 2005. "A New and Effective Method for Optimal Splitting of Total Transmission Ratio of Three Step Bevel-Helical Gearboxes." In *The Sixth Vietnam Conference on Automation*, 175-80, Hanoi.

[8] Pi, V. N., and Dac, V. Q. 2005. "Optimum Calculation of Transmission Ratios for Helical-Worm Reducers." *Journal of Science and Technology, Thai Nguyen University* 4 (36): 70-3.

[9] Pi, V. N., Thao, T. T. P., and Thao, L. T. P. 2015. "A New Study on Optimum Determination of Partial Transmission Ratios of Mechanical Driven Systems Using a V-belt and Two-Step Helical Gearbox." *Vietnam Mechanical Engineering Journal* 10: 123-5.

[10] Chat, T., and Le Van Uyen, D. 1998. "Calculus of Mechanical Transmissions." *Educational Republishing House, Hanoi*.

Journal of Environmental Science and Engineering A
Volume 6, Number 7, July 2017
David Publishing Company
616 Corporate Way, Suite 2-4876, Valley Cottage, NY 10989, USA
Tel: 1-323-984-7526, 323-410-1082; Fax: 1-323-984-7374, 323-908-0457
http://www.davidpublisher.com, www.davidpublisher.org
environmental@davidpublishing.org, environmental@davidpublishing.com

ISSN 2162-5298